



THE EFFECTS OF VEGETATIVE CANOPIES
ON ATMOSPHERIC DISPERSION

THESIS

John R. Lindell, Captain, USAF

AFIT/GEE/ENP/95D-05

DEPARTMENT OF THE AIR FORCE
AIR UNIVERSITY
AIR FORCE INSTITUTE OF TECHNOLOGY

Wright-Patterson Air Force Base, Ohio

DTIC QUALITY INSPECTED 1

AFIT/GEE/ENP/95D-05

THE EFFECTS OF VEGETATIVE CANOPIES
ON ATMOSPHERIC DISPERSION

THESIS

John R. Lindell, Captain, USAF

AFIT/GEE/ENP/95D-05

Approved for public release; distribution unlimited

19960426 045

THE EFFECTS OF VEGETATIVE CANOPIES
ON ATMOSPHERIC DISPERSION

John R. Lindell, B.S., M.S.

Captain, USAF

Approved:

Clifton E Dungey 30 Nov 95
Capt Clifton E. Dungey, Chairman

Edward E Heyse 1 DEC 95
Major Edward E. Heyse

Dennis W Quinn 1 DEC 95
Dr. Dennis W. Quinn

AFIT/GEE/ENP/95D-05

THE EFFECTS OF VEGETATIVE CANOPIES
ON ATMOSPHERIC DISPERSION

THESIS

Presented to the Faculty of the School of Engineering

Air Education and Training Command

In Partial Fulfillment of the

Requirements for the Degree of

Master of Science in Environmental and Engineering Management

John R. Lindell, B.S., M.S.

Captain, USAF

December 1995

Approved for public release; distribution unlimited

Acknowledgment

I would like to thank all of the people who made this effort possible. A great big thank you to Captain Cliff Dungey for your guidance and patience with my journeyman plodding through atmospheric sciences. Another thanks to Professor Jerome Clemmens of Wright-State University, without whose equipment, data, and insight would have made this effort impossible. Thanks again, Jerome for all of the other pertinent information on the Cedar Bog that made every trip out there a great experience, with the exception of the one trip in August when we were attacked by the swarms of mosquitoes at sites three and five. To Dr. Dennis Quinn for the instructions in atmospheric transport and the talks about boating, happy sailing and I hope you enjoy the new Jeep. And to Major Edward Heyse for stepping in and filling an ENV void, I am grateful that you did not turn me away an my hour of need. Thanks for your patience in reading this thesis even though it is outside of your area.

To Karen whose understanding and care made me keep my sanity throughout this program, I am in your debt forever.

Table of Contents

	Page
Lists of Figures	v
Lists of Tables.....	vii
Abstract.....	viii
I. Introduction	
General Issues	I-1
The Gaussian Model	I-2
Atmospheric Stability	I-2
Pasquill-Gifford Stability Scheme	I-3
Problem Statement	I-4
Site Description and Equipment	I-5
Data Collection Sites.....	I-6
Academic Justification.....	I-6
Practical Justification.....	I-7
II. Background	
Overview.....	II-1
Pasquill-Guifford Stability Criteria.....	II-1
Standard Deviation of Wind Fluctuations.....	II-3
Various Comparative Studies	II-4
Effects of Forest Canopies	II-5
III. Methodology	
Overview.....	III-1
Analysis of Field Data.	III-1
Reconstruction of Missing Data.....	III-2
Time Averaging of Data	III-3
Pasquill-Gifford Stability Classes.....	III-9
Pasquill-Gifford Stability Criteria.....	III-10

	Page
Sigma Theta Stability Criteria	III-12
Program STABASC.F	III-13
Industrial Source Complex Short Term Model.....	III-14
IV. Results	
10 Meter Site Parameters	IV-1
1 Meter Site Parameters	IV-18
Comparison of Sites.....	IV-29
Comparison to Previous Experimentation	IV-36
V. Conclusions	
Stability Methods	V-1
Averaging Methods.....	V-2
Airborne Dispersal	V-3
Recommendations.....	V-3
Appendix A: ISCST Input and Output Files.....	A-1
Bibliography	BIB-1
Vita.....	V-1

List of Figures

Figure	Page
1.1	Gaussian Distribution I-2
3.1	Ground Level Solar Radiation: Clear Skies III-11
4.1	Average Wind Direction Frequencies For 10 Meter Data..... IV-2
4.2	Normalized Average Wind Direction Frequencies 10 Meter IV-4
4.3	Average 10 Meter Wind Speed Cumulative Distribution IV-5
4.4	Site 2 10 Meter Stability Distribution IV-6
4.5	Site 4 10 Meter Stability Distribution IV-7
4.6	Site 5 10 Meter Stability Distribution IV-7
4.7	Average Period Concentrations For Site 2 10 Meter Data IV-11
4.8	Average Period Concentration Ratio For Site 2 10 Meter Data IV-12
4.9	Average Period Concentration For Site 5 10 Meter Data..... IV-13
4.10	Average Period Concentration Ratios For Site 5 10 Meter Data IV-14
4.11	Average Period Concentrations For Site 4 10 Meter Data IV-16
4.12	Average Period Concentration Ratio For Site 4 10 Meter Data IV-17
4.13	Average Wind Direction Frequencies 1 Meter Data IV-19
4.14	Normalized Average Wind Direction Frequencies 1 Meter Data..... IV-20
4.15	Average Wind Speed Distributions For 1 Meter Data IV-21
4.16	Site 2 1 Meter Stability Distribution IV-22
4.17	Site 4 1 Meter Stability Distribution IV-23
4.18	Site 5 1 Meter Stability Distribution IV-23

4.19	Average Period Concentrations For Site 2 1 Meter Data	IV-25
4.20	Average Period Concentration Ratios For Site 2 1 Meter Data	IV-26
4.21	Average Period Concentrations For Site 5 1 Meter Data	IV-27
4.22	Average Period Concentration Ratios For Site 5 1 Meter Data	IV-28
4.23	Average Period Concentrations For Site 4 1 Meter Data	IV-30
4.24	Average Period Concentration Ratios For Site 4 1 Meter Data	IV-31
4.25	Comparison of Sites Using Pasquill-Gifford Method 10 Meter Data	IV-33
4.26	Comparison of Sites Using σ_θ Method 10 Meter Data.....	IV-33
4.27	Average Period Concentration Ratio For All Sites 10 Meter Data	IV-34
4.28	Average Concentration Ratio For All Sites 1 Meter Data.....	IV-35
4.29	Stability Frequencies At Site 4 10 Meter Data.....	IV-38

List of Tables

Table	Page
1.1 Pasquill-Gifford Stability Scheme.....	I-3
2.1 Pasquill-Gifford Stability Criteria.....	II-3
3.1 Pasquill-Gifford Stability Classes.....	III-10
3.2 Pasquill-Gifford Stability Criteria.....	III-10
3.3 Boundary Values For Incoming Solar Radiation.....	III-12
3.4 Modified Mitchell Method Criteria.....	III-13
4.1 10 Meter Wind Speed Statistics.....	IV-5
4.2 Summary Statistics For σ_θ Values.....	IV-9
4.3 Comparison of σ_θ Values.....	IV-38

Abstract

This research was conducted to improve our understanding of the effects of vegetative canopy-induced turbulence on the dispersion of air pollution. The computer model most often used to calculate atmospheric dispersion is the Gaussian plume model, which requires some method to compute the downwind dispersion coefficients. These coefficients are a parameterization of the atmospheric stability or the level of turbulence in the atmosphere. The Environmental Protection Agency's recommended parameterization scheme is the Pasquill-Gifford method. By comparing the Pasquill-Gifford method to the Modified Mitchell method using σ_θ , the standard deviation of the horizontal wind fluctuations, the relative precision of each method is determined and their effects on a Gaussian model can be seen. Contrasting three sites with varying levels of vertical obstructions, the most effective method of measuring the turbulence level was determined to be the σ_θ method. The meteorological data show that the wind direction fluctuates up to 50% more in a forested area when compared to an open field. This larger value translates to an increase in atmospheric turbulence at the forested site. In addition, the resulting output of the Gaussian model showed the forested site having a 3.5 times greater concentration than the open field, showing the effects of the increased turbulence and channeling of wind flow introduced by the forest canopy.

The Effects of Vegetative Canopies on Atmospheric Dispersion

I. Introduction

1.1. *General*

The National Ambient Air Quality Standards (NAAQS) were established to maintain or improve the quality of air within the United States. The Prevention of Significant Deterioration (PSD) stipulations within the Clean Air Act (CAA) require that the air quality in regions that are cleaner than the criteria presented in the NAAQS remain that way. In order to introduce new sources of air pollution accompanying new industries or processes, the new sources are not allowed to increase the total emissions in that area. The need to predetermine the impact of these new sources on the ambient air quality in the region has made air pollution modeling a necessary part of every new action involving emissions to the atmosphere.

The scientific modeling of air pollutants were initially driven by warfare. The introduction of poison gas in World War One led defense establishments of countries to investigate how particles are transported in the atmosphere. To maintain a lethal concentration of agent in an area, the amount of dispersion of the agent by the atmosphere had to be determined. The factors that govern the dispersion were primarily determined to be the wind speed and the level of turbulence in the atmosphere. Whereas the wind speed could be measured directly, the measurement of turbulence present in the atmosphere has always been determined by indirect measurements. It is precisely this

lack of direct measurement of turbulence level that has led to much scientific effort being devoted to develop a means of quantifying the turbulence level using common atmospheric parameters.

1.2. *The Gaussian Model*

The standard air pollution model for point source is the Gaussian model. The Gaussian model assumes a normal distribution of particles in the lateral and vertical directions.

The distribution has a mean μ which occurs at the centerline of the plume and 68% of the particles fall within a distance of one standard deviation σ in each direction (see

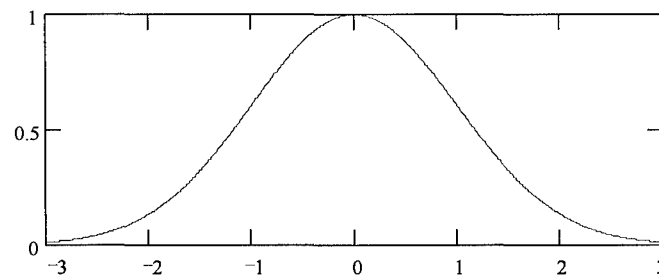


Figure 1.1 Gaussian Distribution

Figure 1.1). The greater the value of the standard deviation, the greater the width of the plume, i.e., the more the particles have dispersed. The Environmental Protection Agency defines the plume as being situated along the x axis and is from a continuous source at steady state (Turner, 7).

1.3. *Atmospheric Stability*

Atmospheric stability is a euphemism for turbulence level in the atmosphere.

Unstable atmospheric conditions have low wind speeds and large eddies that increase the dispersive nature of the atmosphere due to the increased turbulence. These large eddies

are introduced by the convective heating of the air by the ground as the ground is heated through incoming solar radiation. Neutral conditions have high wind speeds and small to medium eddies present. These eddies are typically mechanical turbulence which are introduced by vertical obstructions in the flow of the wind such as trees or buildings. A stable atmosphere has little or no turbulence and is characterized by near-laminar flow with small eddies, slow wind speeds, and near isothermal or inverted temperature profiles causing the turbulent eddies to be small.

1.4. *Pasquill-Gifford Stability Scheme*

The most commonly used stability scheme is the Pasquill-Gifford classification that uses alphabetical groupings of stability conditions from A (most unstable) through D (neutral) to F (stable). Condition G, very stable, was added at a later date to balance the classification. Numerous methods have been developed using different atmospheric parameters to attempt to determine the correct Pasquill-Gifford stability classification present in the atmosphere. Each of these methods is still a general approximation of the turbulence level and in areas of great induced turbulence, such as a forest, these methods are still lacking proof of their applicability.

TABLE 1.1

PASQUILL-GUIFFORD STABILITY SCHEME

Stability	A	B	C	D	E	F	G
	Very Unstable	Unstable	Mod. Unstable	Neutral	Mod. Stable	Stable	Very Stable

1.5. *Problem Statement*

This thesis effort was undertaken to investigate stability classification methods within vegetative areas. Little research has been conducted on this subject, with most previous research in atmospheric stability occurring over smooth surfaces. Rough and irregular surfaces such as forest canopies induce greater turbulence levels, causing greater dispersion of the particles. Contrasting the stability classification methods with smooth surfaced sites and a rough site will lead to a greater understanding of the effects of rough terrain on the different methods. Two different stability criteria systems will be used: the Pasquill-Gifford method and the standard deviation of the horizontal wind fluctuations (σ_θ method).

In addition, the area of time averaging of data will be explored. Most meteorological parameters such as wind velocity, direction, and temperature are gathered on an hourly basis. However, these values are either are the values present on the hour or averaged from intermediate readings. The former is the case in meteorological information gathered by human observers. In the case of the latter, which is common in meteorological data collection stations for experiments, there are a few methods to change the time scale on data to go from X minute averaged data to Y minute averaged data. For scalar values such as temperature and wind speed, simple averages are the rule. However, in the case of average wind fluctuations, the intermediate variances are lost. A new method was derived based on statistical relationships that will be contrasted with an accepted method, the power law.

1.6. *Site Description and Equipment*

The Cedar Bog is a nature preserve 25 miles north of Springfield, Ohio. The area is composed of 315 acres of hardwood trees and cedars of varying heights with interspersed areas of marsh and prairie. The bog is surrounded by farm fields growing primarily corn. The State of Ohio Department of Transportation (ODOT) has sited a future expansion of US Route 68 to extend northward from Springfield to Urbana, OH, that passes within one mile of the bog. As part of that expansion, ODOT contracted with Wright State University to conduct an environmental assessment on air and ground water quality impacts due to road construction and increased vehicular traffic.

As part of that study, five 10-meter meteorological towers were installed in the southeast, southwest, northeast, and northwest corners of the bog, forming a rough parallelogram, and one station in a partial clearing in the center of the bog. Each tower has a 3-cup anemometer, wind vane, a fast response thermocouple probe, and a humidity sensor on a protruding arm at 10 meters, 5 meters, 2 meters, and 1 meter; all connected to a datalogger in an enclosure at the base of the tower. In addition, the southeastern tower has a pyranometer to measure solar intensity, atmospheric pressure sensor, and a tipping bucket rain gauge. The instruments were interrogated every one second for readings for horizontal wind velocity, horizontal wind direction, standard deviation of wind direction, temperature, and relative humidity for each height. In addition, the tower at site 1 recorded 15 minute averages of solar radiation, atmospheric pressure, and rainfall. The datalogger stores 15 minute averages of the data into a storage module. The 15 minute averaged data used in this effort stretches from 14 April 1995 to 9 July 1995.

1.7. *Data Collection Sites*

Data from the towers at sites 2, 4, and 5 were used in this study. Site 2 is primarily smooth, with an open farm field on its east side and open prairie on the other three sides. No vertical obstructions are within 500 feet of the tower. Site 4 is on the northeast corner and is characterized by having an open prairie on three sides, with a single line of trees running east and west on its north side. Its distance from the end of the bog tree line is over 500 feet. Site 5 is in a small clearing in the heart of the bog and is characterized by cedar and small hardwood trees on all four sides, with larger hardwood trees on its southwest side.

1.8. *Academic Justification*

Investigating the aspects of induced turbulence will aid to make further advances in the area of air pollution modeling. The primary focus is to contrast two accepted methods of determining stability: an older method (Pasquill-Gifford) using indirect sensing of turbulence and a newer method (the modified σ_θ method) using direct sensing of turbulence. With the benefit of better instrumentation, the more accurate method of directly measuring the wind fluctuations (σ_θ method) can be used to determine the relative accuracy of the older Pasquill-Gifford method that relied upon common meteorological parameters. Other studies in turbulent areas that do not have the σ_θ measurement can then be judged on their relative accuracy and its effects on the output of a Gaussian model.

In addition, the derived method of time-averaging data might prove to be more accurate than the power method in time-averaging standard deviations. If this is the case, the newer method will capture more of the variance from the original data. The resulting more accurate determination of the wind fluctuations will lead to an increase in accuracy in the use of the sigma theta method.

1.9. *Practical Justification*

The practical benefits from this experiment are two-fold. First, the Air Force has installations or operations that are surrounded by forests. At some time, air pollution regulations might require modeling of the dispersion from emissions on the installation, typically from aircraft that are operating on the ground. The weather station on an installation will only record hourly measurements of basic meteorological parameters, typically not including the standard deviation of the wind direction. Being forced into determining atmospheric stability from a method other than the sigma theta method will introduce a great deal of error into the Gaussian model. This experiment will give an estimate of the relative effect of the different methods of determining stability on the model's output.

The second usable feature of this thesis is in the area of estimating relative concentrations of particles in terrain that surrounds forests. A general idea of the effect of the amount of induced turbulence and its effect on the dispersion of particles can be attained by contrasting the model's output at site 2 with sites 4 and 5. This information can be useful in biological/chemical warfare to help decide the relative contamination of

sites. If the forested areas provide a faster dispersion of contaminants, it would follow that the forested areas would drop to a lower concentration level before open terrain.

II. Background

2.1 Overview

The search to accurately measure the stability of the atmosphere has led to diverse methods to use weather parameters to characterize turbulence levels. Early efforts used estimates of turbulence levels (standard deviation of wind fluctuation) that were difficult to measure in real time, leading to research into pairing stability with commonly recorded weather criteria such as mean wind speed, cloud cover, gust level, and incoming solar intensity. With the advancement of technology, the new focus of research is to use direct measurements of turbulence to accurately reflect the stability level of the atmosphere.

2.2 Pasquill-Gifford Stability Criteria

G. I. Talyor's (1921) statistical analysis of the distribution of particles in an airborne plume assumed that the turbulent field was not dependent upon time and position. Cramer (1957) followed by relating the distribution of the airborne particles to a Gaussian distribution with lateral dispersion coefficient σ_y and vertical dispersion coefficient σ_z . Following the *Prairie Grass* experiments, Cramer, et al. (1959) published various parameter values for dispersion over a smooth field at varied atmospheric conditions at downwind distances from 1 meter to 1000 meters.

Further analysis by Hay and Pasquill (1959) at the Chemical Defense Experimental Establishment revealed that dispersion in the surface boundary layer was dependent upon varying levels of turbulence in the atmosphere that were characterized as σ_y (horizontal) and σ_z (vertical), the angle of the spread of the plume from the point of

release. For numerous experiments over flat fields, the spreads of the plume at downwind distances of less than 1000 meters were approximated by the following relationship:

$$\sigma_y/x \approx (\sigma_\theta)_{\tau,x/u} \quad (2.1)$$

where σ_y is the horizontal dispersion angle, x is the downwind distance, σ_θ is the standard deviation of the horizontal wind direction over release duration time τ at the time determined by dividing the position downwind x by the mean wind speed u . For elevated releases, vertical distribution of particles was found to be:

$$\sigma_z/x \approx (\sigma_\phi)_{\tau,T} \quad (2.2)$$

where σ_z is the vertical dispersion angle, x is the downwind distance, σ_ϕ is the standard deviation of the vertical wind fluctuations at duration of release τ and over averaging period T . A common lack of means to determine σ_θ and σ_ϕ led Pasquill (1961) to relate the ambient atmospheric conditions to commonly measured weather parameters such as cloud cover, incoming solar radiation, and mean surface winds (see Table 2.1).

Gifford (1961) related Pasquill's observations of the standard deviation of the plume spread to concentration dispersion coefficients within the plume itself. However, these values were applicable only over smooth terrain with surface roughness factors (z_0) less than 1 cm. Turner (1969) published these values in a widely used Workbook of Atmospheric Dispersion Estimates.

TABLE 2.1

PASQUILL-GIFFORD STABILITY CRITERIA

Surface Wind Speed (at 10 m)	Insolation			Night		Stability Conditions
	Strong	Moderate	Slight	Thinly overcast or $\geq 4/8$ low clouds	$\leq 3/8$ clouds	
m/sec						
<2	A	A-B	B	-	-	A-Very unstable B-Moderately unstable
2-3	A-B	B	C	E	F	C-Slightly stable
3-5	B	B-C	C	D	E	D-Neutral
5-6	C	C-D	D	D	D	E-Moderately stable
>6	C	D	D	D	D	F-Stable

2.3 Standard Deviation of Wind Fluctuations

Cramer's (1957) and Pasquill's (1961) preferred method of determining turbulence levels was to measure σ_θ and σ_ϕ directly. Lack of widely available equipment to measure those parameters led them to other methods. However, as advancements in electronics led to computerized recording equipment, agencies took a new look at an old idea. Pasquill and Smith (1971) revisited his earlier methods in light of several demonstrations of the performance of wind fluctuation models and extended his original dispersion estimates to longer ranges, greater surface roughness lengths, and elevated sources. Gifford (1968) suggested that the Pasquill stability classes could be determined directly by σ_θ . The Nuclear Regulatory Commission (formerly the U.S. Atomic Energy Commission, 1968) adopted the temperature lapse rate ($\Delta T/\Delta Z$) and σ_θ to characterize turbulence on a real-time basis for modeling effluent release from nuclear power plants. Pasquill (1976) again made another argument for using σ_θ to accurately portray the atmospheric conditions in data for Gaussian models. Mitchell and Timbre (1979) point

out the usefulness of the σ_θ method for recording weather data. Previous methods relied on cloud cover recordings that were typically only taken at a small number of locations, usually distant from the site of interest. In addition, Mitchell and Timbre provide modified σ_θ criteria for day and night conditions to take into account for plume meandering at low wind speeds at night. Yamartino (1984) developed a theory to calculate single pass estimators of σ_θ that yielded a means of reducing data storage requirements and allowed remote recordings of atmospheric stability data. Turner (1985) tested three different methods for calculating σ_θ and found that Yamartino's method gave the best results, well within Yamartino's published range of $\pm 2\%$ accuracy. Yamartino's method is now the EPA's accepted method of calculating the ten minute averaged σ_θ values.

2.4 Various Comparative Studies

Numerous research efforts have been directed towards the search to resolve the question of which estimator of atmospheric stability yields the most accurate results. Draxler (Draxler, 1976) explored the results of varied averaging times for different methods (temperature lapse rate, Richardson's number, σ_θ) for ground and elevated sources. He suggested that the horizontal dispersion parameters are underestimated for elevated sources in stable conditions and vertical dispersion parameters are overestimated in unstable conditions. Sedefian and Bennet (1980) concluded after testing 10 methods (forms of temperature lapse rate, Richardson's number, and σ_θ) with the EPA Regional Air Monitoring model (EPA, 1979) that the Richardson's number methods appeared to

give the best results. However, the model used dispersion over flat terrain and the authors acknowledged that the Richardson's number method in rougher terrain would yield unrealistic conclusions. Sedefian and Bennet endorsed the method proposed by Irwin (1979) of calculating the dispersion coefficients directly would be useful rather than taking the intermediate step of determining atmospheric stability.

Mitchell (1982) tested four methods (temperature lapse rate, σ_θ , modified σ_θ for meandering plumes, Pasquill-Gifford) for short term dispersion estimates from a ground level source. The modified σ_θ approach was found to give the best dispersion estimates. Irwin (1983) tested four approaches to characterizing the dispersion parameters and found that Draxler's (1987) approach best approximated data from the *Prairie Grass* and *Karlsruhe* experiments. Four stability schemes (temperature lapse rate, σ_θ , Richardson's number, Turner) were evaluated by Draxler (1987) over Washington, D.C.. Draxler reported that the σ_θ method had the least biased estimates when the calculated values were compared to measured values. The precision of all four methods were identical.

2.5 *Effects of Forest Canopies*

An acknowledged fact from most studies is that the Pasquill-Gifford curves are inadequate for determining dispersion variables for plumes in complex surfaces and with low wind speeds. Bowne (1974) expounds that the Pasquill-Gifford dispersion coefficient curves are suitable only for flat terrain and forwarded three dispersion curves for use in urban areas that adjusted the surface roughness from smooth to rough. That the Pasquill-Gifford curves underestimate the concentration close to the source and

overestimate the concentration further downwind in rough terrain was stated by Miller (1978). He advocated the use of the Smith-Briggs curve which minimized the errors of the Pasquill-Gifford curves in rough terrain, but even this method did not match the empirical data.

Little research has been accomplished in plume dispersion in forest canopies and with induced mechanical turbulence. McNeal (1983) stated that the forest-atmosphere boundary layer must be evaluated as a continuum, linking the air flow in the forest with the lower atmosphere. Cionco (1985) explored that coupling of the mesoscale and microscale meteorological variables and parameters to build a model that will predict the penetration and dispersion of an airborne particle into a forest canopy. Pinker and Holland (1988) researched the effect of induced turbulence on atmospheric stability. Values for σ_0 were determined and were found to be greater by 20% to 100% in the clearing than when compared to previous studies over smoother fields. In addition, the values of σ_0 over the forest canopy were 50% greater than those in the clearing, clearly indicating the effect of the induced mechanical turbulence of the forest canopy on the boundary layer.

III. Methodology

3.1. Overview

The Cedar Bog project was initiated by the Ohio Department of Transportation in accordance with the National Environmental Policy Act to study the potential effects of the expansion of US Route 68 from Springfield to Urbana, OH. Five meteorological towers were placed in and around the bog with a station in each corner and a station in the center of the bog. Previous data from the bog indicated a seasonal prevailing southwesterly wind. With this prevailing wind, the data from sites 2, 4, and 5 were chosen for this study to trace the effect of the tree canopy in the turbulence level of the surface boundary layer.

3.2. Analysis of Field Data

The data provided by the field sensors are 15 minute averages of 1 second readings with the exception of the wind direction and the wind direction standard deviation. Data gathered between April 15, 1995 and July 8, 1995 were chosen for the study. Previous to April 15, numerous equipment failures prevented data collection at site 5. Windspeed sensor failure at site 4 capped the collection of data at July 8.

Scalar quantities temperature, barometric pressure, solar intensity, and wind speed were averaged over 15 minutes by the dataloggers. The 15 minute averaging time was selected for use with Pasquill-Gifford stability criteria. The unit vector mean wind direction was averaged by the following formula:

$$\theta = \text{Arc tan}(S_a/C_a) \quad (3.1)$$

where the x vector component s_a , the y vector component c_a , and n number of observations are:

$$S_a = \frac{\sum_{i=1,n} \sin \theta_i}{n} \quad \text{and} \quad C_a = \frac{\sum_{i=1,n} \cos \theta_i}{n} \quad (3.2a \ \& \ b)$$

Yamartino's algorithm (Yamartino, 1984) was used to attain the average σ_θ . Most estimators use two passes of the data set to calculate σ_θ , the first pass to establish the mean and a second pass to calculate the deviance from the mean. Yamartino's "single-pass" estimator of σ_θ approximates the mean with each addition of a wind angle and then calculates σ_θ by the following formulation:

$$\sigma_\theta = \sin^{-1}(\varepsilon)(1+b\varepsilon^3) \quad (3.3)$$

where b is equal to $\left(\frac{2}{\sqrt{3}} - 1\right)$ or 0.1547. ε is defined as:

$$\varepsilon \equiv 1 - \left(s_a^2 + c_a^2\right) \quad (3.4)$$

where s_a and c_a are from equation 3.2a and b. Through 100 Monte Carlo simulations of equation 3.3, Yamartino observed no significant mean bias in his algorithm and had an estimated error of no more $\pm 2\%$ when compared to true σ_θ values. Yamartino's algorithm was verified by Turner who determined a 1.5% error estimate in true and calculated σ_θ values in his own data sets.

3.3. *Reconstruction of Missing Data*

Missing data points occurred at only nine instances within the data set due to equipment maintenance at the data collection sites. To maintain the structure of four

atmospheric readings per hour for the atmospheric stability determination program, the missing data points were reconstructed by using straight line interpolation between the previous and following data points. For 15 minute period, this method can be deemed accurate for scalar quantities of pressure, solar radiation, temperature, and relative humidity. However, for the mean wind direction, mean wind speed, and σ_θ , this method loses considerable accuracy, but at the present time, no other method of data reconstruction exists for these quantities.

3.4. *Time Averaging of Data*

A two day period of one minute averaged data was collected for use in another research effort. That data had to be converted to conform to the standard 15 minute averaged data set. The temperature, relative humidity, solar radiation, barometric pressure, and mean wind speed were averaged through a simple summation:

$$\text{average} = \frac{\sum_{i=1,15} X_i}{15} \quad (3.5)$$

However, the mean wind direction and σ_θ again posed a challenge. Without ϵ from equation 3.3, the variance of the series is lost, and there was no way found to reconstruct the one minute-averaged ϵ from the one minute-averaged σ_θ values from equation 3.3.

To solve this problem, two approaches were taken. A theoretical approach using the unbiased estimator of the standard deviations of a series of numbers was derived. For this example, 15 minute-averaged data will be transformed to 60 minute-averaged data (4 time periods).

$$\sigma_1 = \sqrt{\frac{\sum_{N_1} (x - \mu_1)^2}{N_1}} \quad (3.6)$$

The expression is squared and expanded to yield:

$$\sigma_1^2 = \frac{\sum_{N_1} (x^2 - 2x\mu_1 + \mu_1^2)}{N_1} \quad (3.7)$$

Expanding the summation to sum each term individually yields:

$$\sigma_1^2 = \frac{\sum x^2}{N_1} - \frac{\sum 2x\mu_1}{N_1} + \frac{\sum \mu_1^2}{N_1} \quad (3.8)$$

Since the mean μ and the square of the mean μ^2 are constants, the average of constants are the constants, μ and μ^2 can be brought out of the summation.

$$\sigma_1^2 = \frac{\sum x^2}{N_1} - 2\mu_1 \frac{\sum x}{N_1} + \frac{N\mu_1^2}{N_1} \quad (3.9)$$

Simplifying 3.9 and recognizing that $\frac{\sum x}{N_1}$ is μ_1 , solving 3.9 for $\sum x^2$ gives:

$$\sum x^2 = N_1(2\mu_1^2 - \mu_1^2 + \sigma_1^2) \quad (3.10)$$

which simplifies to:

$$\sum x_1^2 = N_1(\mu_1^2 + \sigma_1^2) \quad (3.11)$$

Executing equations 3.7 to 3.11 for series two through series 4 yields:

$$\sum x_2^2 = N_2(\mu_2^2 + \sigma_2^2) \quad (3.12a)$$

$$\sum x_3^2 = N_3(\mu_3^2 + \sigma_3^2) \quad (3.12b)$$

$$\sigma_{\text{grand}} = \sqrt{\frac{1}{P} \left[\sum_{n=1}^4 \sigma_n^2 \right] + \frac{1}{P} \mu_1^2 + \frac{1}{P} \mu_2^2 + \frac{1}{P} \mu_3^2 + \frac{1}{P} \mu_4^2 - \mu_{\text{grand}}^2} \quad (3.19)$$

The square of the grand mean is separated into 1/P sections $\left[\frac{1}{P} (\mu_{\text{grand}}^2) \right]$ and grouped with each individual time period mean and summed to form:

$$\sigma_{\text{grand}} = \sqrt{\frac{1}{P} \left[\sum_{n=1}^4 \sigma_n^2 \right] + \frac{1}{P} \left[\sum_{n=1}^4 \mu_n^2 - \mu_{\text{grand}}^2 \right]} \quad (3.20)$$

The portion of equation 3.20 that is not capable of being calculated with the data in the database is the differences in the square of the mean wind directions for the individual time periods and the square of the grand mean of the wind direction or

$\frac{1}{P} \left[\sum_{n=1}^4 \mu_n^2 - \mu_{\text{grand}}^2 \right]$. The value that can be calculated from the data base is the summation

of the squares of the differences in the individual means and the grand mean or

$\sum_P (\mu_i - \mu_{\text{grand}})^2$. The solution is to determine if are equivalent statements as shown in

equation 3.20.

$$\frac{1}{P} \left[\sum_P (\mu_i^2 - \mu_{\text{grand}}^2) \right] = \sum_P (\mu_i - \mu_{\text{grand}})^2 \quad (3.20)$$

The invocation of the central limit theorem (Devore, 218) can attain that goal. Expanding

the summation of $\sum_P (\mu_i - \mu_{\text{grand}})^2$ yields:

$$\left[\sum_P (\mu_i^2 - \mu_{\text{grand}}^2) \right] = \left(\sum_P \mu_i^2 - \sum_P 2\mu_i \mu_{\text{grand}} + \sum_P \mu_{\text{grand}}^2 \right) \quad (3.21)$$

Expanding the summation on the left side of equation 3.21 will yield:

$$\sum_P \mu_i^2 - \sum_P \mu_{\text{grand}}^2 = \sum_P \mu_i^2 - \sum_P 2\mu_i \mu_{\text{grand}} + \sum_P \mu_{\text{grand}}^2 \quad (3.22)$$

Equation 3.22 is true only if $\sum_P -2\mu_i \mu_{\text{grand}} + \sum_P \mu_{\text{grand}}^2 = \sum_P -\mu_{\text{grand}}^2$. Grouping the grand mean summations on the right hand side of the equation will produce:

$$\sum_P -2\mu_i \mu_{\text{grand}} = -2\sum_P \mu_{\text{grand}}^2 \quad (3.23)$$

Realizing that the grand mean (μ_{grand}) is a constant, this value can be pulled outside of summation on the left hand side of the equation. On the right hand side of the equation, the square of the grand mean (μ_{grand}^2) is constant, and n summations of a constant is equal to n times the constant, equation 3.23 can be rewritten as:

$$-2\mu_{\text{grand}} \sum_P \mu_i = -2(P)\mu_{\text{grand}}^2 \quad (3.24)$$

Dividing each side by the time period yields the final equation:

$$-2\mu_{\text{grand}} \frac{\sum_P \mu_i}{P} = -2\mu_{\text{grand}}^2 \quad (3.25)$$

Invoking the central limit theorem (Devore, 218) which states that given a random sample of X_i 's, the distribution can be assumed to be normal with a mean of μ as long as n is sufficiently large. In this case, there is a distribution of means μ_i 's with each mean μ representing the average of 900 readings (15minutes*60readings/minute), n is sufficiently

large, so the grand mean μ_{grand} is approximated by $\frac{\sum_P \mu_i}{P}$. Making this substitution in equation 3.25 gives:

$$-2\mu_{\text{grand}}^2 = -2\mu_{\text{grand}}^2 \quad (3.26)$$

which proves that over a series, equation 3.22 is true.

$$\left[\sum_P (\mu_i^2 - \mu_{\text{grand}}^2) \right] = \sum_P (\mu_i - \mu_{\text{grand}})^2 \quad (3.22)$$

Substituting the relationship developed in equation 3.22 into equation 3.18 will give resulting equation 3.27 that enables the new standard deviation to be calculated:

$$\sigma_{\text{grand}} = \sqrt{\frac{1}{P} \left[\sum_{n=1}^4 \sigma_n^2 \right] + \frac{1}{P} \left[\sum_{n=1}^4 (\mu_n - \mu_{\text{grand}})^2 \right]} \quad (3.27)$$

The squares of the standard deviation terms can be summed over P time periods to give the final form of the equation:

$$\sigma_{\text{grand}} = \sqrt{\frac{1}{P} \left(\sum_{i=1}^P \sigma_i^2 \right) + \frac{1}{P} \sum_{i=1}^P (\mu_i - \mu_{\text{grand}})^2} \quad (3.28)$$

In order to use this method, the grand mean wind direction μ_{grand} must be calculated. The average wind directions in the smaller time increments are summed as vector components over the total number of time periods P.

$$x_{\text{comp}} = \sum_P \cos(\theta - 270) \quad \text{and} \quad y_{\text{comp}} = \sum_P \sin(\theta - 270) \quad (3.29a \text{ and } b)$$

The vectors are averaged over the number of readings to find the average x_{comp} and the average y_{comp} .

$$\bar{x}_{\text{comp}} = x_{\text{comp}}/P \quad \text{and} \quad \bar{y}_{\text{comp}} = y_{\text{comp}}/P \quad (3.30a \text{ and } b)$$

The resulting average wind direction is found.

$$\mu_{\text{grand}} = \arctan \left[\frac{\bar{x}_{\text{comp}}}{\bar{y}_{\text{comp}}} \right] \quad (3.31)$$

A second approach to finding the new time-averaged σ_θ is the use of the power law. The power law states that the time base for a value can be changed through an exponential relationship between the two time values as the distribution of mean values and averaging times is logarithmic. The value of the exponential in the relationship between the averaging times is 0.2.

To change the σ_θ value from a 15 minute averaged value to a 60 minute averaged value, the following equation is used:

$$\sigma_{60} = \sigma_{15} \left[\frac{60}{15} \right]^{0.2} \quad (3.32)$$

where the σ_{15} value is the simple average of the four 15 minute-averaged standard deviations. Both of these approaches will be used to calculate a 60 minute averaged σ_θ value, and the results of the methods will be compared to each other and their resulting effects on stability parameterization.

3.5. *Pasquill-Gifford Stability Classes*

The Pasquill-Gifford stability classes range from A through G as shown in Table 3.1. Horizontal and vertical coefficients of dispersion are determined from charts developed by Pasquill based upon these values that are determined by various means.

TABLE 3.1

PASQUILL-GIFFORD STABILITY CLASSES

Pasquill-Gifford Stability classes	A	B	C	D	E	F	G
Atmos. Condition	Very Unstable	Unstable	Mod. Unstable	Neutral	Mod. Stable	Stable	Very Stable

3.6. *Pasquill-Gifford Stability Criteria*

Pasquill-Gifford stability criteria are based upon readily measured atmospheric conditions such as solar inclination and wind speed as shown in Table 3.2. To determine insolation level for hourly readings, the solar altitude and cloud layer is necessary but not available in this data base. However, using a scheme developed by Kasten and Czeplak as mentioned by Holtslag and van Ulden (1983), the surface fluxes can be derived based

TABLE 3.2

PASQUILL-GIFFORD STABILITY CRITERIA

Surface Wind Speed (at 10 m)	Insolation			Night		Stability Conditions
	Strong (>60°)	Moderate (>35° and <60°)	Slight (<35°)	Thinly overcast or ≥ 4/8 low clouds	≤3/8 clouds	
m/sec						
<2	A	A-B	B	-	-	A-Very unstable B-Moderately unstable
2-3	A-B	B	C	E	F	C-Slightly unstable
3-5	B	B-C	C	D	E	D-Neutral
5-6	C	C-D	D	D	D	E-Moderately stable
>6	C	D	D	D	D	F-Stable

on the approximate latitude of Cedar Bog. Using a simple parameterization of the incoming solar radiation based on the latitude of the area of interest, an estimate for the

maximum (clear skies) values for each hour is calculated according to the following formula:

$$K_0^+ = a_1 \sin \phi + a_2 \quad (3.33)$$

where K_0^+ is the incoming solar radiation at ground level under clear skies, ϕ is the solar elevation, and a_1 and a_2 are empirical coefficients that are related to the location of the site. Of the five sets of coefficients given by Holtslag and van Ulden for various

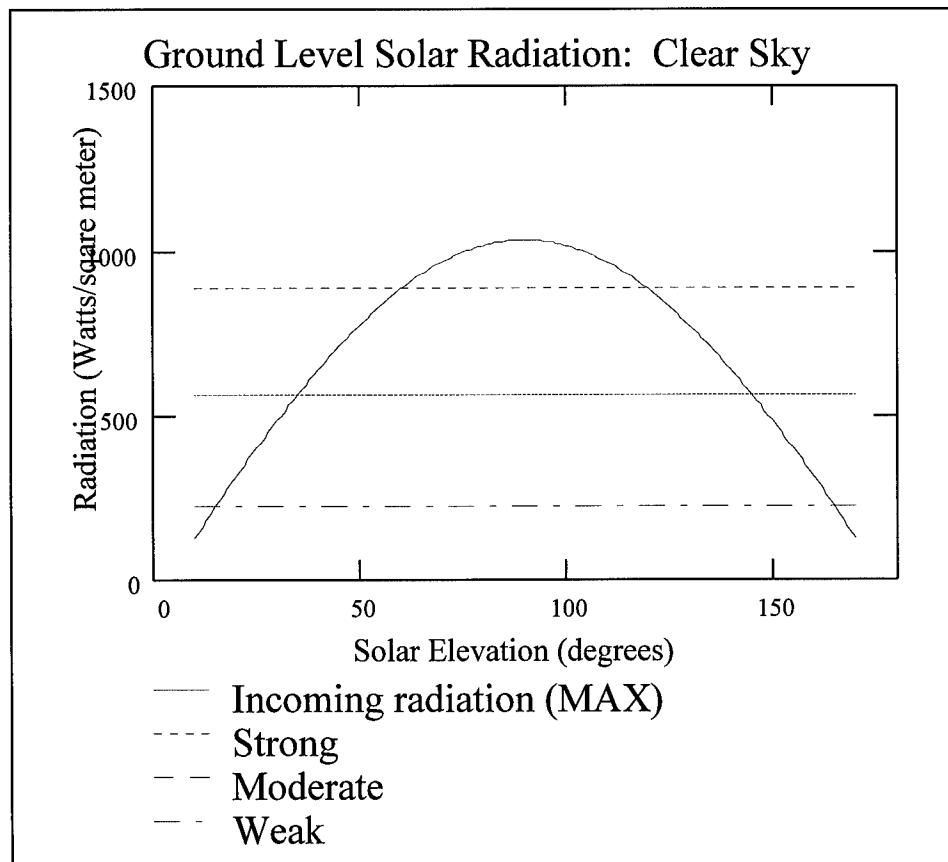


Figure 3. 1

latitudes, the coefficients for Boston, MA ($a_1 = 1098 \text{ Watts/m}^2$ and $a_2 = -65 \text{ Watts/m}^2$) have the greatest similarity to the Cedar Bog due to their similar latitudinal position.

equation 3.33 to calculate the maximum incoming solar radiation based on solar elevations (angle from eastern horizon to the sun) from 10° to 170° for a full daytime cycle, cutoff values were determined as shown in Table 3.3 from the Figure 3.1.

TABLE 3.3
BOUNDARY VALUES FOR INCOMING SOLAR RADIATION

	Strong	Moderate	Weak
Solar angle in degrees	60° - 120°	35° - 60° 120° - 155°	10° - 35° 155° - 170°
Upper Value in W/m^2	N/A	885	580
Lower Value in W/m^2	885	580	219

3.7. σ_{θ} Stability Criteria

The use of Mitchell's modified σ_{θ} method was implemented in program STABASC.F as discussed in section 3.8. Using the values of σ_{θ} generated by the power law and the derived empirical method, the criteria for the Pasquill-Gifford stability parameters breaks the values into two major time periods: day and night. Night is defined as lasting one hour before sunset to one hour after sunrise, and day is the rest of the time. Using the value of the incoming solar radiation to determine the status of day or night (less than $50 W/m^2$ is night) and the respective one hour average of the wind speed, the criteria in Table 3.6 were used to determine the stability conditions for the 10 meter and 1 meter heights at each condition and each σ_{θ} averaging method.

TABLE 3.4

MODIFIED MITCHELL METHOD CRITERIA

Stability	Day		Night			
	σ_{θ}		σ_{θ}		average wind speed	
	upper	lower	upper	lower	upper	lower
A	none	<22.5	none	>22.5	>2.4	none
B	22.5	17.5	22.5	>22.5 17.5	2.9 2.4	2.4 none
C	17.5	12.5	22.5 17.5	>22.5 17.5 12.5	3.6 3.0 2.4	2.9 2.4 none
D	12.5	7.5	none 22.5 17.5	>22.5 17.5 12.5	N/A none none	>3.6 <3.0 <2.4
E	7.5	3.8	7.5	3.8	none	none
F	3.8	2.1	3.8	2.1	none	none
G	>2.1	none	>2.1	none	none	none

3.8. Program STABASC.F

In order to calculate the data required by air pollution model, program STABASC.F was developed. The program takes 15 minute average readings from an input file from each site, and computes one hour averaged data by the methods mentioned in section 3.4. From this one hour averaged data, three Pasquill-Gifford stability classifications are generated by the two stability criteria: Pasquill-Gifford and Modified σ_{θ} with two types of inputs. The criteria are output into a file for each site in the format required for input into ISCST. In addition, the program zones the average wind direction into 16 different zones of 22.5° starting at 0° corresponding to the receptor zones. The last information output by the program is a frequency distribution of the average wind speed into 0.5 meter/sec increments.

3.9. Industrial Source Complex Short Term (ISCST) Model

The model used to test the effects of the stability parameters was the ISCST model. The ISCST model uses the following straight-line, steady-state Gaussian Plume equation to model simple point source emissions from stacks over short time periods and calculates point receptor concentrations or receptor averages:

$$\chi = \frac{Q}{2\pi\sigma_y\sigma_z u_s} \exp\left[-0.5\left(\frac{y}{\sigma_y}\right)^2\right] \quad (3.34)$$

where χ is the concentration in grams per cubic meter, Q is the source term in grams per second, σ_y is the lateral dispersion coefficient, σ_z is the vertical dispersion coefficient, u_s is the mean wind speed in meters per second, and y is the distance from the centerline in meters.

The model uses polar or Cartesian coordinate receptor centers where the origin is X_0 and Y_0 and the coordinates of a receptor are given by the following coordinates:

$$X(R) = r \sin(\theta) - X_0 \quad \text{and} \quad Y(R) = r \cos(\theta) - Y_0 \quad (3.35)$$

The downwind distance from the source, given by coordinates $X(S)$ and $Y(S)$, to the receptor along the direction of plume travel is given by:

$$x = -(X(R) - X(S)) \sin(WD) - (Y(R) - Y(S)) \cos(WD) \quad (3.36)$$

where WD is the direction from which the wind is blowing. The crosswind distance y to the receptor from the plume centerline is given by:

$$y = (X(R) - X(S)) \cos(WD) - (Y(R) - Y(S)) \sin(WD) \quad (3.37)$$

ISCST lets the user categorize emission sources into three basic categories: point, area, and volume. Upper wind data files from meteorological station readings from the

National Weather Service of the same time period of interest are utilized to characterize the regional upper air conditions. Surface layer conditions are input via a ASCII II file that contains atmospheric parameters from the site of interest. The parameters fed into the program are the year, month, day, hour, flow vector, wind speed, temperature, stability parameter, rural mixing height, and urban mixing height for each hour of data.

To test the effects of the different stability methods on each site and to determine the effects of the tree canopy on atmospheric dispersion, two main runs were made of ISCST for each site. The first run is for an elevated source—a 100 meter stack—and the second run is for a ground level emission. Each emission source is the same, 10 grams per second of SO₂. Ten meter data of average wind speed, σ_{θ} , and average wind direction were used in the elevated plume and 1 meter data were used in the ground release plume. A polar coordinate receptor grid was specified and kept the same for each run: every 22.5° at a radius of 500 meters from the source, for a total of 16 zones and 16 receptors. The receptors are at ground level and the maximum 3 hour, 24 hour, and average period concentrations are output for each receptor. A copy of a typical input and output file is in Appendix A.

IV. Results

4.1. 10 Meter Site Parameters

4.1.1. Wind Data. The averaged wind direction data produced significant insight into the physical parameters of the different sites. Figure 4.1 shows the frequency distribution for all three sites at the 10 meter level. For the 93 day period, distributions of the average hourly wind direction show that the wind is primarily from the south in all sites, varying from south-southeast at site 2 to the south at site 5. Surprisingly, a sizable percentage of the wind was also found to be from the north. Of interest in the chart is the pairing of relative peaks in site 5's wind distribution associated with clearings in the forest: a clearing northwest of the tower corresponds to the peak at 348° and a large clearing due south of the tower adds to the maximum at zone 180° in addition to the prevailing wind direction.

On Figure 4.1, site 2 has a greater frequency of wind from the north than do sites 4 and 5, but site 4 has more wind from the south and the northeast, and site 5 has winds from the northwest and from the south. This disparity in wind directions can partially be explained by the location of the bog to these sensor stations. A southeasterly breeze will be measured by site 2 which is in the open, but this same breeze is probably channeled in the bog due to the heavier vegetation to become more of a southern breeze at site 5. Site 4 has more obstructions on its eastern side so the flow is diverted by obstacles in the wind's path. The clearing on the northwestern side of site 5 explains why that site has a greater frequency of winds from the northwest than do sites 2 and 4, which both experience the same frequency of winds in that direction.

Average Wind Direction Frequencies 10 Meter Data

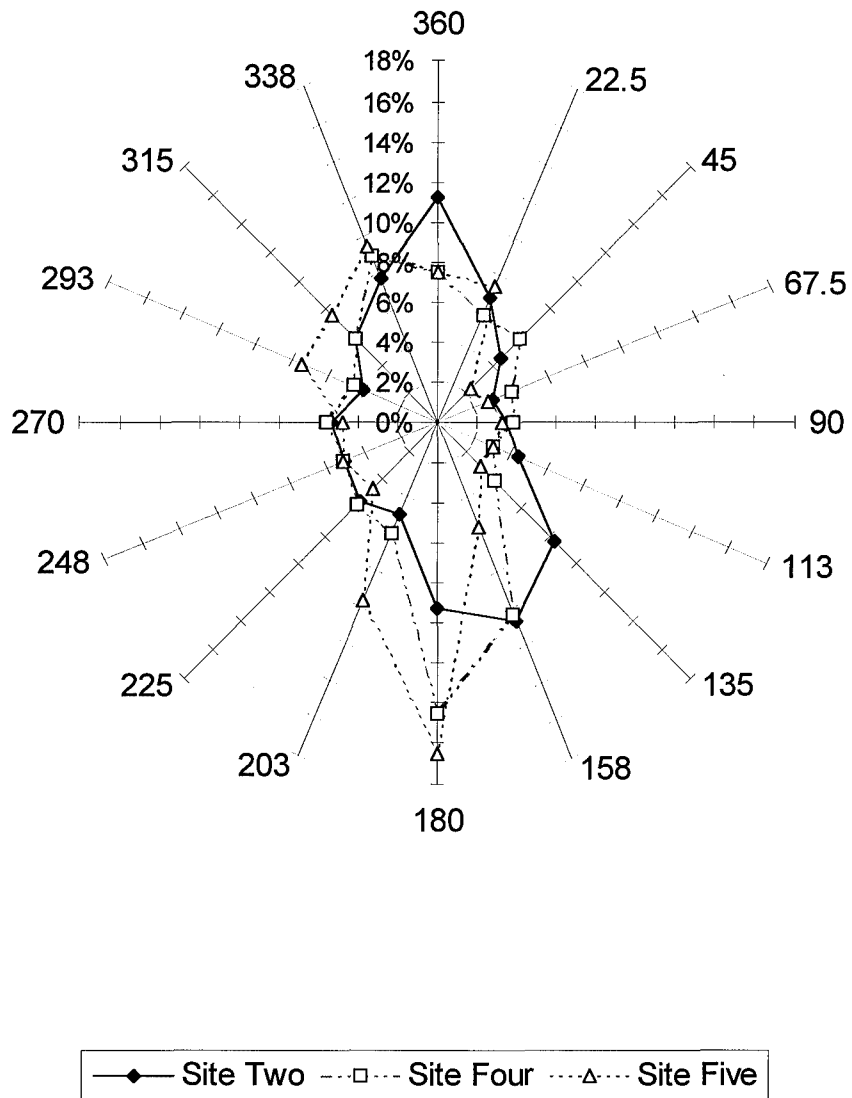


Figure 4.1 Average Wind Direction Frequencies For 10 Meter Data

Figure 4.2 shows the wind direction frequencies normalized to site 2. Site 2 is viewed as the unobstructed site, the true wind direction frequency distribution. Site 5 is the site with the greatest amount of vegetative canopy and vertical obstructions, with site 4 lying in-between the two sites in terms of vertical obstructions, but being closer to open characteristics of site 2. Site 5 has the greatest differences in wind direction frequencies, with site 4 being in better agreement with site 2. The differences in the wind direction frequencies at sites 4 and 5 when compared to site 2 can be attributed to the effects of the vegetation of the bog, which deflects and channels the wind as the wind penetrates the bog canopy.

Figure 4.3 is the average wind speed cumulative distribution data for all three sites at the 10 meter height. Again, the effects of the vegetative canopy can be seen by comparing the wind speed at site 2 to sites 4 and 5. Site 2 is viewed as the true wind speed distribution due to its open nature. The wind speeds at site 2 are higher than the other sites in terms of maximum and average speed. The wind speeds at site 5 are the slowest, with its distribution being over half of site 2's range of values. The distribution at site 4 again lies between the two but closer to site 2 due to the similarities of sites 2 and 4.

Table 4.1 shows some descriptive statistics for the sites' 10 meter average wind speeds. As expected, the highest wind speeds are found in the site with the most open area around it, site 2. It is interesting to note that the wind speeds at site 4 are less than that of site 2. Site 4 is relatively open but downwind of the bog in terms of the prevailing wind direction. A common rule of thumb is that the effects of a vertical

**Normalized Average Wind Direction Frequency
Distribution
10 Meter Data**

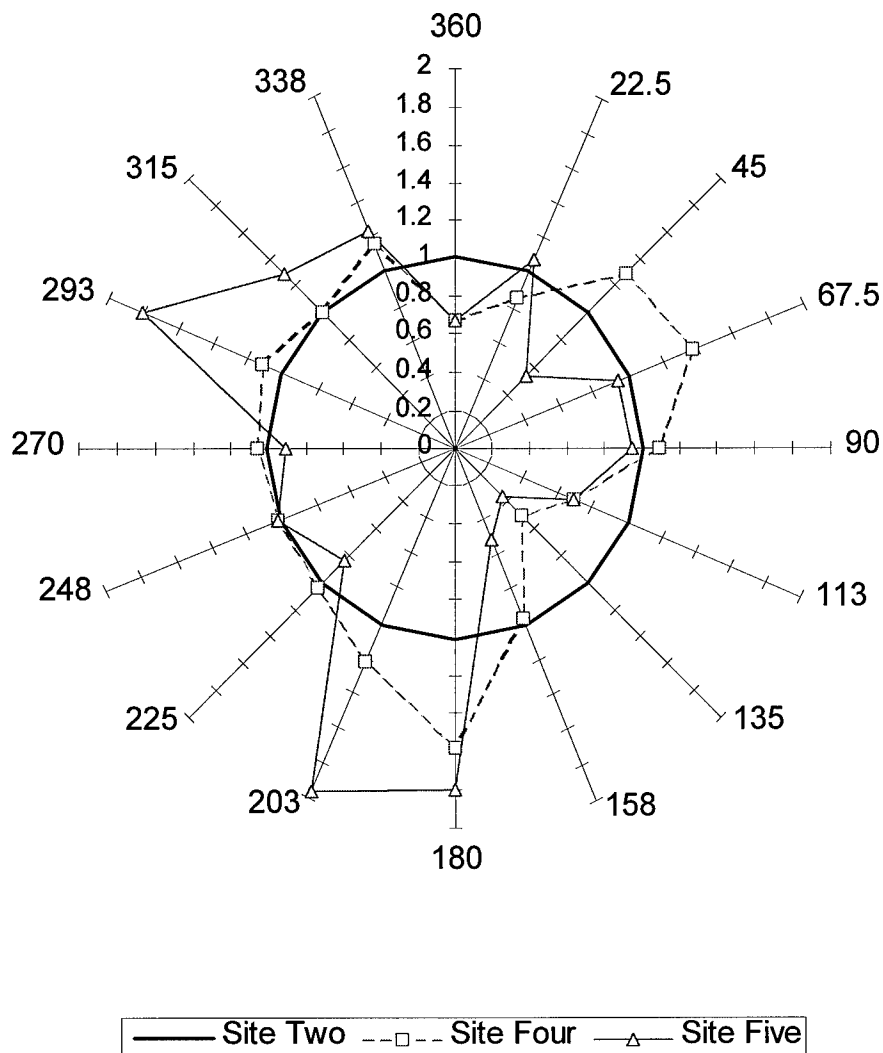


Figure 4.2 Normalized Wind Direction Frequencies For 10 Meter Data

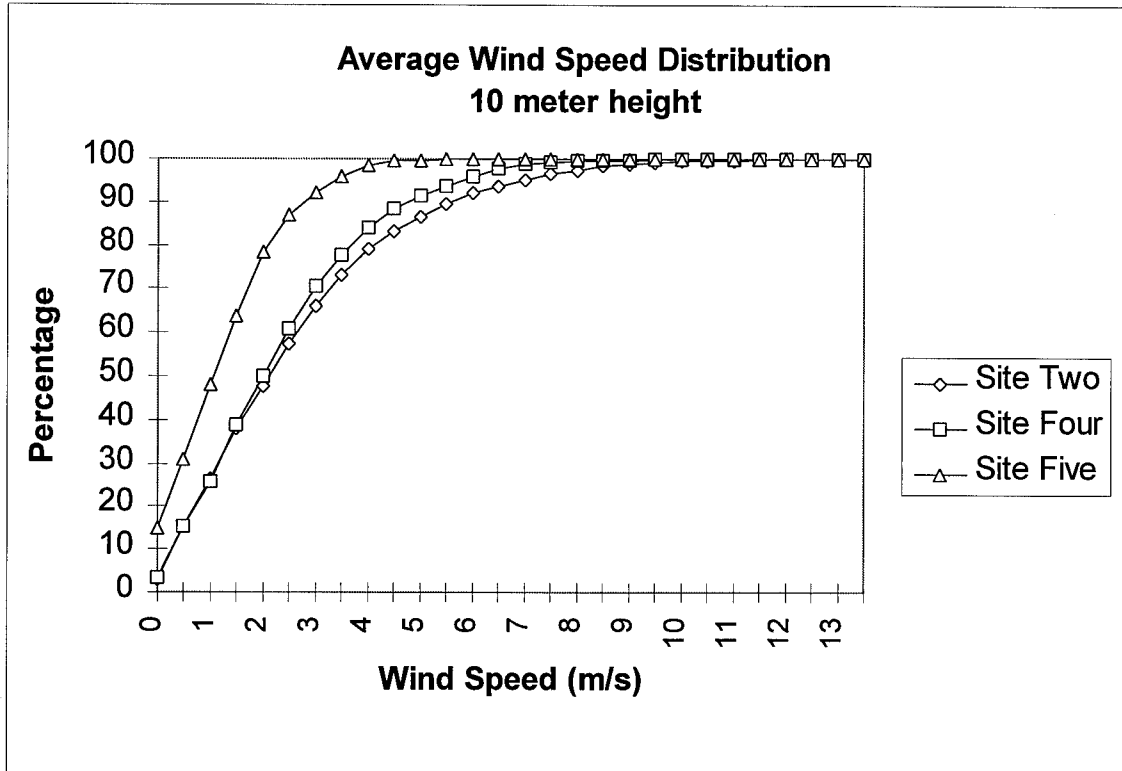


Figure 4.3 Average 10 Meter Wind Speed Cumulative Distribution

downwind obstruction are not “felt” by a sensor that is located at a distance downwind 10 times the height of the obstruction. It appears that site 4 is still experiencing some effects of the vegetative canopy which is approximately 60 feet tall at its maximum although the tower is at least 500 feet from the end of the bog tree line. Site 5, being a relatively sheltered spot, has the lowest wind speeds, which shows the deflection of the wind up and over or around the bog and a slowing of any wind that penetrates the canopy.

TABLE 4.1

10 METER WIND SPEED STATISTICS			
Site	2	4	5
Mean	2.81	2.54	1.45
Standard Deviation	2.12	1.74	1.12
Minimum	0	0	0
Median	2.5	1	.5
Maximum	13.5	11	6.5

4.1.2. Stability Classification Distribution. The frequency distributions of the stability conditions are shown in Figures 4.4 to 4.6 for each site at the 10 meter level. The Pasquill-Gifford (P-G) criteria is compared to the two σ_0 methods to show the effects of the vegetation on the two different types of stability classification schemes, indirect and direct sensing of turbulence.

The Pasquill-Gifford criteria (P-G) yielded either a very unstable (A) or stable (F) condition over 50% of the time for all three sites, with site 5 having over 75% of the readings at the extreme end of scale. Neutral conditions are most prevalent at site 2 which agrees with the recorded data for that site to have the highest average and peak wind speeds. Neutral conditions rarely occur at site 5, which reflects the sheltered nature of the site in terms of wind speed. Of interest is that the majority of readings were in the stable range (A to C) for each site.

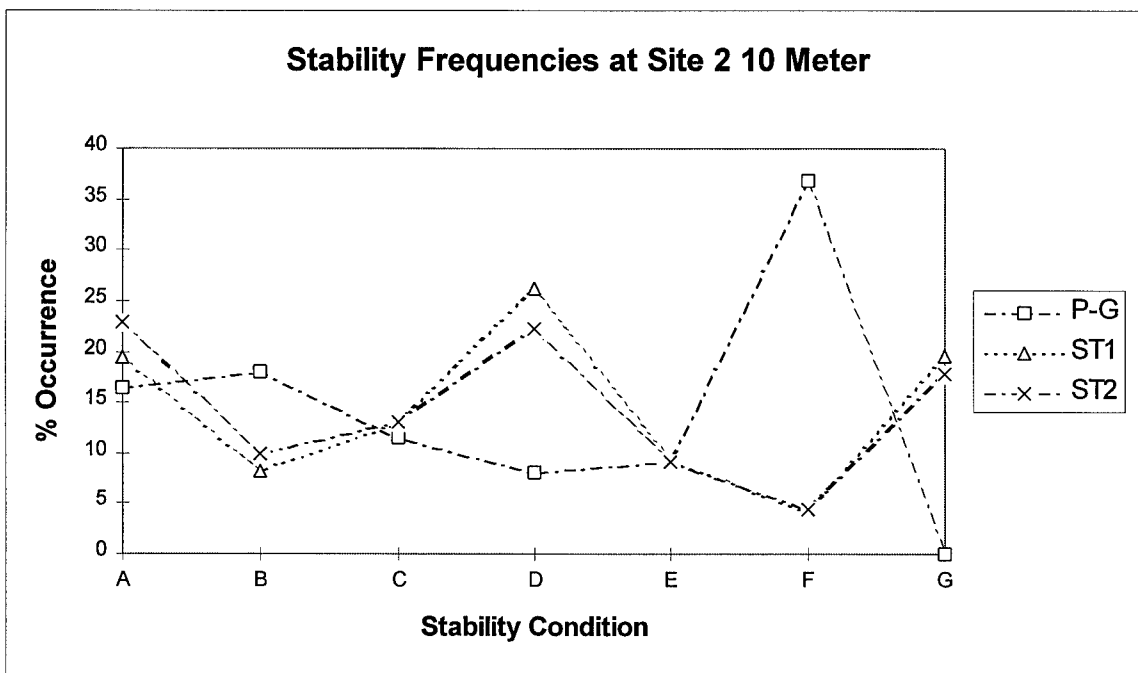


Figure 4.4 Site 2 10 Meter Stability Distribution

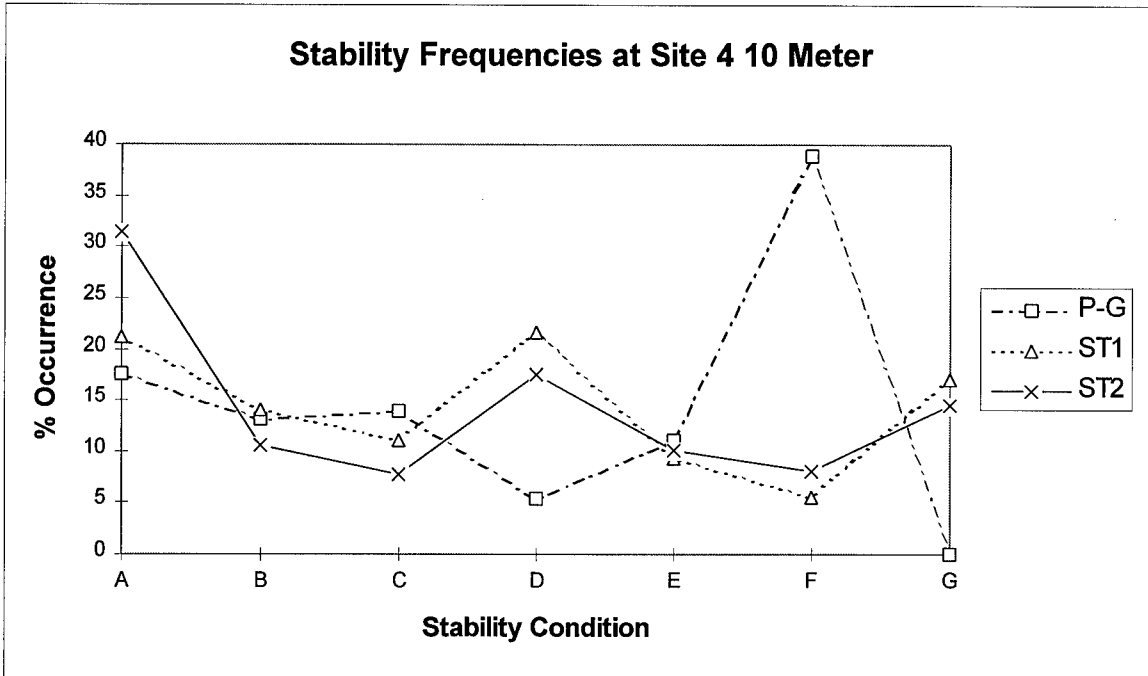


Figure 4.5 Site 4 10 Meter Stability Distribution

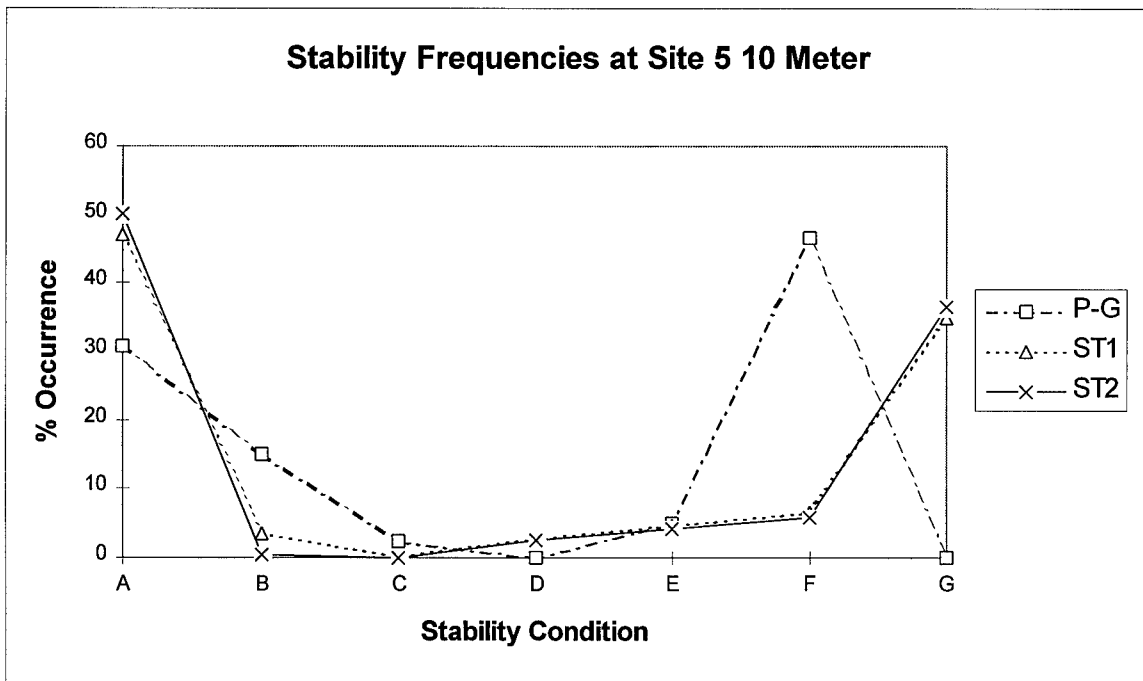


Figure 4.6 Site 5 10 Meter Stability Distribution

Both σ_θ methods gave results that matched the expectations of the sites. At the open sites, sites 2 and 4, the σ_θ methods had a balanced distribution of stability

conditions, where at site 5, a majority of conditions were at the extremes. Sites 2 and 4 yielded almost identical results, which is expected since each site has similar features. A high percentage of the readings for sites 2 and 4 are in the neutral conditions for both types of averaged σ_θ 's which agrees with literature that states flat, open sites should have a large occurrence of neutral conditions. In addition, by reviewing the data for site 2, a large percentage of the very stable condition G occur at night when the wind is from the east. This behavior is indicative of some type of nighttime air drainage from the bog.

The distribution of the stability conditions at site 5 is skewed which reflects the effects of the canopy penetration by the wind. The criteria for the modified Mitchell method gives insight this penetration as the wind diverted and slowed by the numerous objects in its path. The wind has large numbers of induced eddies (mechanical turbulence) which are reflected by large σ_θ values and a large number of very unstable readings. In the case of the large number of stable readings, a weak wind will not have the energy to penetrate the canopy with sufficient force to build eddies. This weak wind results in small σ_θ values and low wind speeds. Extremely fast winds will have the energy to penetrate the canopy with force and to have a more directed flow within the bog, giving high wind speeds and small σ_θ values and neutral conditions. These extremely powerful winds rarely occur and hence only a small percentage of the readings are neutral.

Comparing the results of the different methods of averaging σ_θ at the 10 meter height, the power method consistently produced smaller values of σ_θ for site 2 and 4, but

the opposite is true at site 5 (Table 4.2). However, the variability of the derived method exceeds that of the power method at all sites. This increased variance

TABLE 4.2
SUMMARY STATISTICS FOR σ_θ VALUES

METHOD	Site 2		Site 4		Site 5	
	Derived	Power	Derived	Power	Derived	Power
MEAN	28.40	25.60	27.72	25.60	42.56	44.63
SD	23.22	15.92	20.82	13.77	20.39	18.64
MINIMUM	2.87	3.65	4.00	3.36	0.00	0.00
MEDIAN	18.78	19.70	19.98	22.47	38.14	42.06
MAXIMUM	121.65	102.53	117.47	110.91	121.85	105.56

would indicate that the derived method is retaining a greater measure of the variability from averaging of the 15 minute data. It is also interesting to note the mean values of σ_θ at sites 2 and 4 when compared to site 5. The effect of the induced turbulence due to the surrounding vegetative canopy can be seen by comparing site 5 to site 2 as the variability and values of the fluctuations at site 5 are almost twice that of site 2.

The effects of the two different σ_θ averaging methods on the stability conditions by the modified Mitchell method are negligible at site 5. Discrepancies were most prevalent at the open sites, sites 2 and 4. For the open sites, each method yielded approximately the same number of stable and unstable cases as a whole. However, the power method of σ_θ averaging displayed a tendency to yield more cases of A stability, whereas the derived method of σ_θ averaging gave more cases of G stability.

4.1.3. ISCST Output. The output of the model for the elevated release case at site 2 is shown in Figure 4.7. Figure 4.8 depicts the concentrations normalized to

Pasquill-Gifford method's results to accentuate the differences in the output of the methods. In the western direction, the two σ_θ methods (ST1 is derived and ST2 is power) predict a higher concentration than the Pasquill-Gifford method. This higher concentration can be attributed to the bog which is to the east which imparts some mechanical turbulence to the wind, causing the σ_θ methods to report a greater occurrence of unstable conditions. This greater frequency of unstable conditions will cause a higher ground-level concentration from the elevated plume. However, in the north-south directions, the Pasquill-Gifford method reports a higher concentration due to the greater frequency of unstable conditions in these directions. The σ_θ methods sense a greater frequency of neutral conditions in these conditions. When the wind is from due south, the wind is channeled to the east and west around the bog. The channeling increases the velocity and must dampen some of the turbulence in the wind. The Pasquill-Gifford method cannot sense the dampened turbulence and report unstable conditions when the conditions appear to be actually neutral or near-neutral. At site 5, the concentration curves in Figure 4.9 and 4.10 are similar around the points of the compass. The two σ_θ methods are in agreement with each other with the exception of due north, and these methods report higher concentrations than the Pasquill-Gifford method. At site 5, the amount of mechanical turbulence is the greatest of all the sites. Only the σ_θ methods can sense this mechanical turbulence that occurs in all directions and report a large percentage of the very unstable condition A. The Pasquill-Gifford method cannot detect this

**Average Period Concentration For Site 2
Elevated Release**

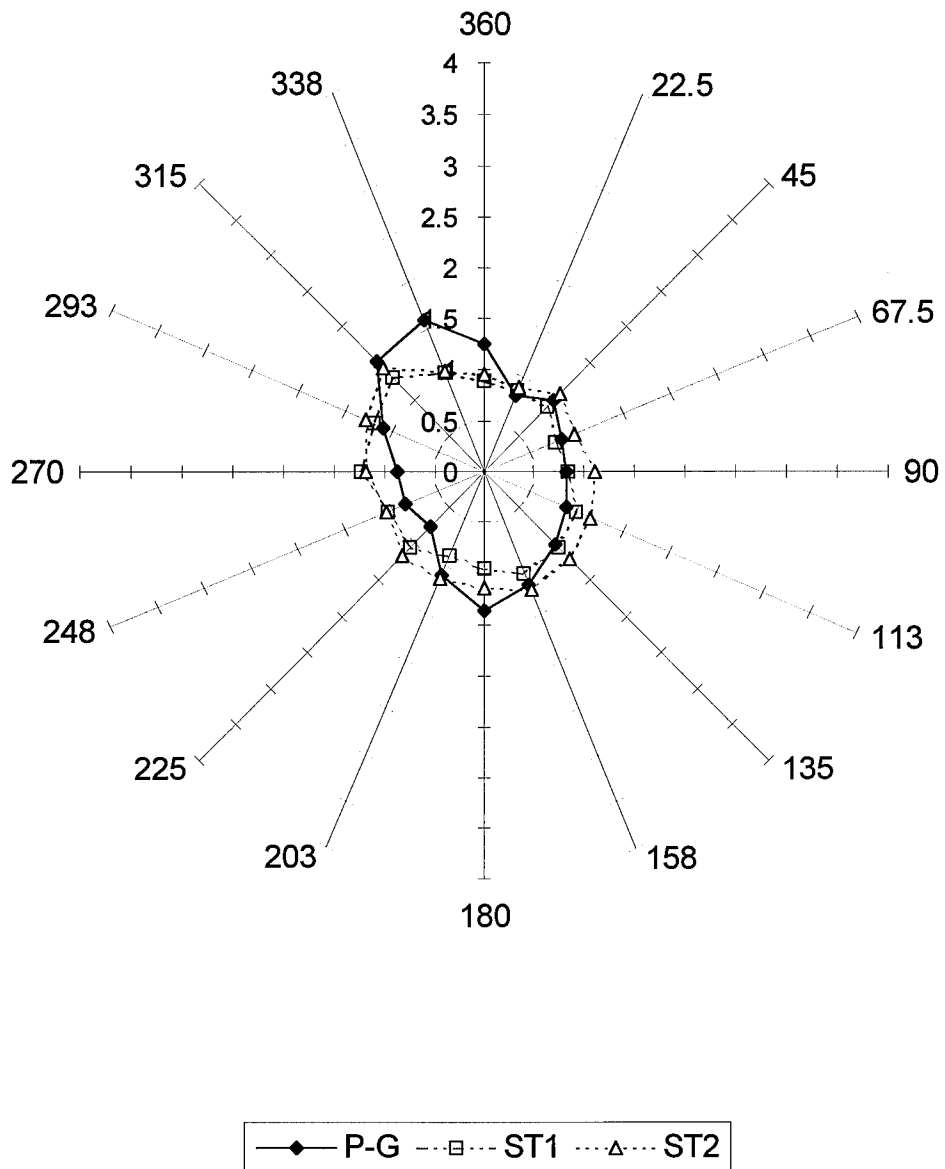


Figure 4.7 Average Period Concentration For Site 2 10 Meter Data

Average Period Concentration Ratio For Site 2 Elevated Release

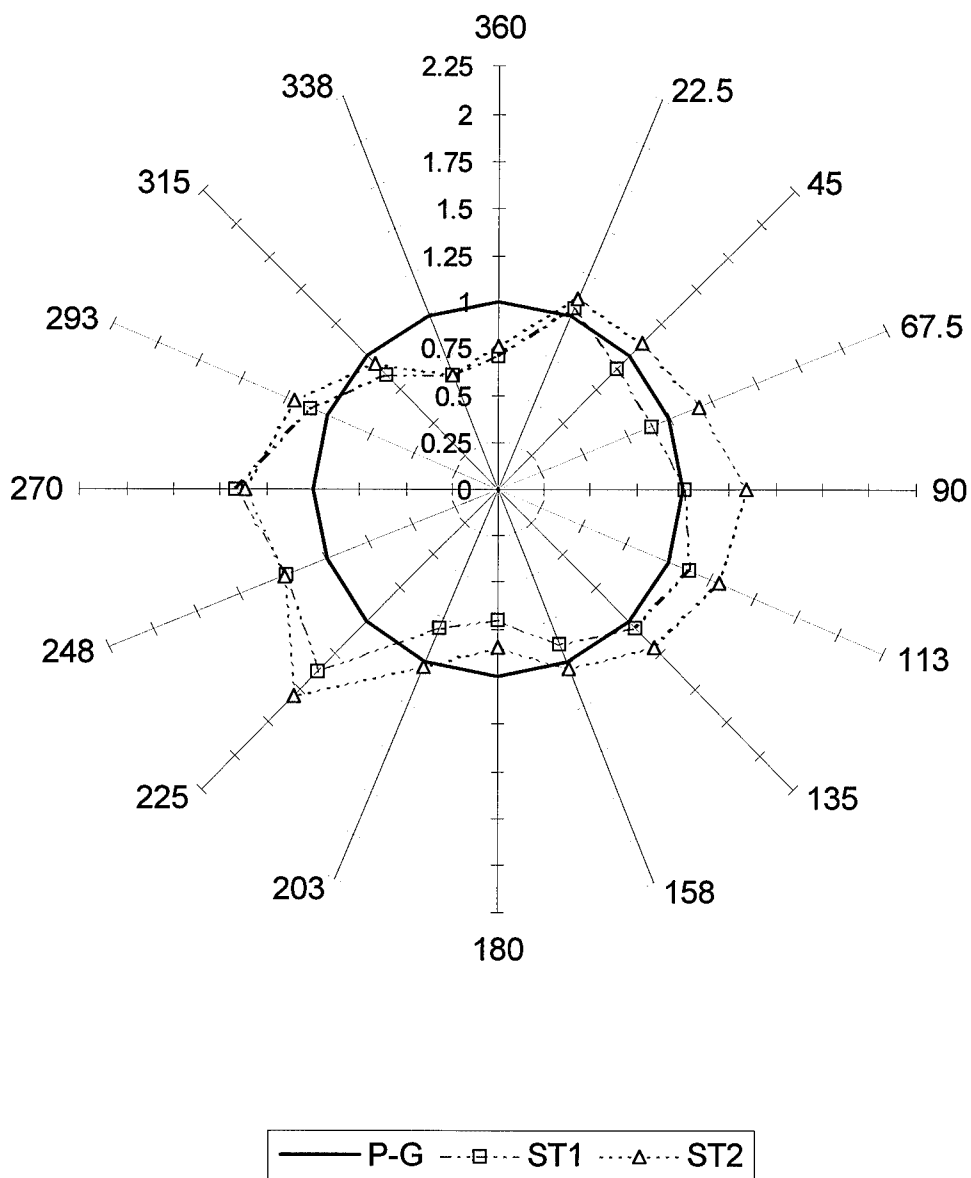


Figure 4.8 Average Period Concentration Ratio For Site 2 10 Meter Data

**Average Period Concentration For Site 5
Elevated Release**

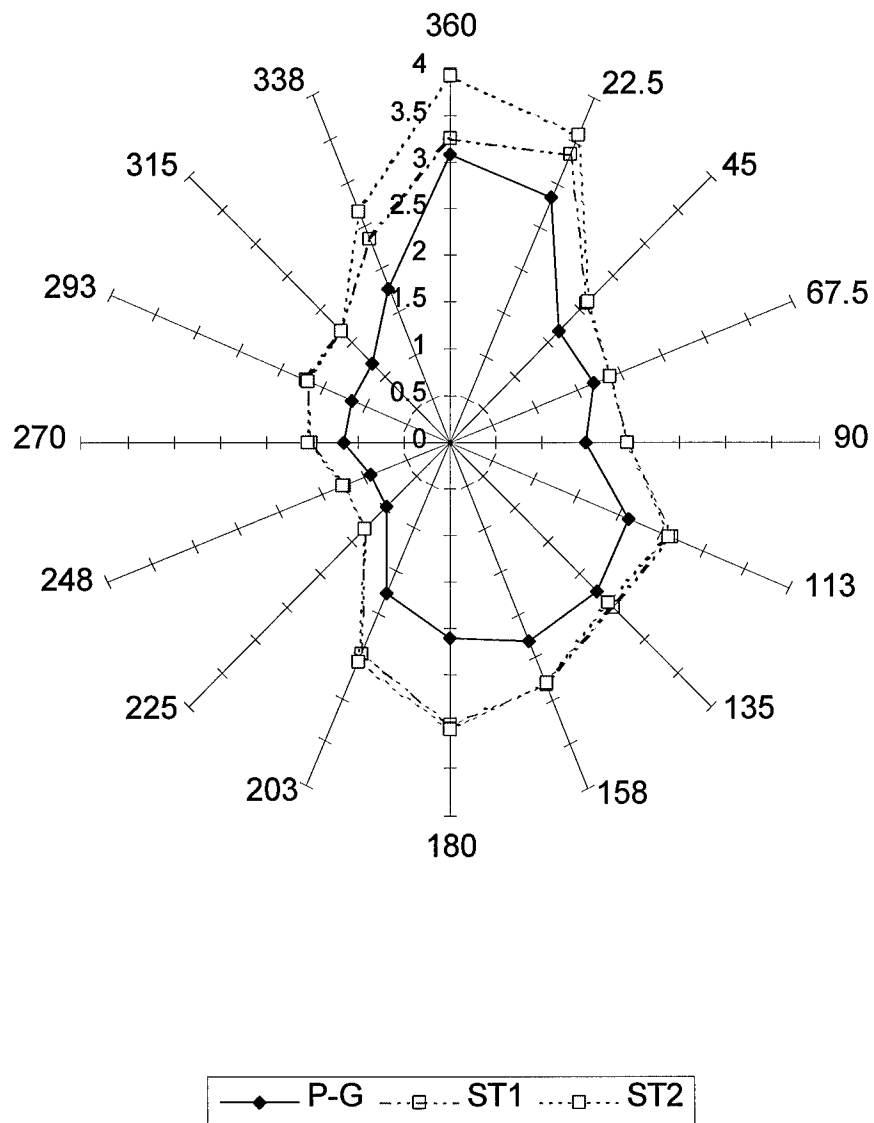


Figure 4.9 Average Period Concentration For Site 5 10 Meter Data

Average Period Concentration Ratios For Site 5 Elevated Release

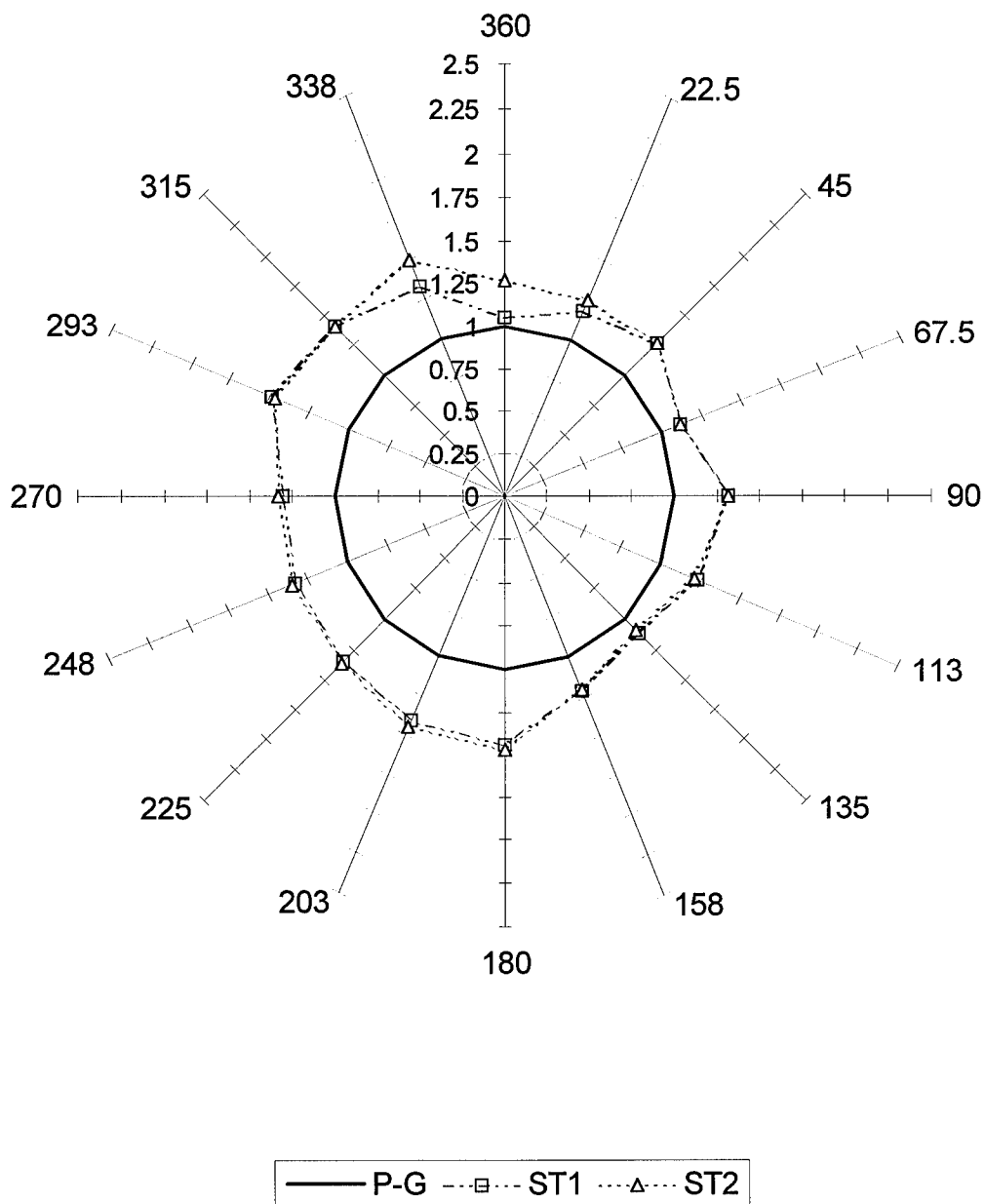


Figure 4.10 Average Period Concentration Ratios For Site 5 10 Meter Data

increases turbulence level and reports a smaller number of unstable conditions, leading to lower concentrations.

Figure 4.11 and Figure 4.12 are the output for site 4. The σ_θ methods have a higher concentration on the eastern side that is due to added turbulence from the bog, which is to the west of this site. When the wind is from the west, the turbulence level in the wind increases due to interaction with the forest canopy in the bog, and the increased mechanical turbulence is detected by the sensors on the tower. This increased turbulence level will yield larger values of σ_θ , which will in turn lead to a greater frequency of unstable conditions. The Pasquill-Gifford method cannot detect this added turbulence, and will report more stable conditions, leading to lower concentrations in the output of the model in the eastern direction. From the shapes of the curves on the eastern side, the methods are reporting similar conditions (unstable), but the degree of the conditions vary. It appears that the power σ_θ method (ST2) is reporting very unstable conditions, the derived σ_θ method (ST1) is reporting moderately unstable conditions, and the Pasquill-Gifford method is reporting slightly unstable conditions. By using Figure 4.5 for the unstable condition A, the power method is reporting a greater frequency of this condition, followed by the derived method, with the Pasquill-Gifford method having the least occurrence of this condition.

Average Period Concentrations For Site 4 Elevated Release

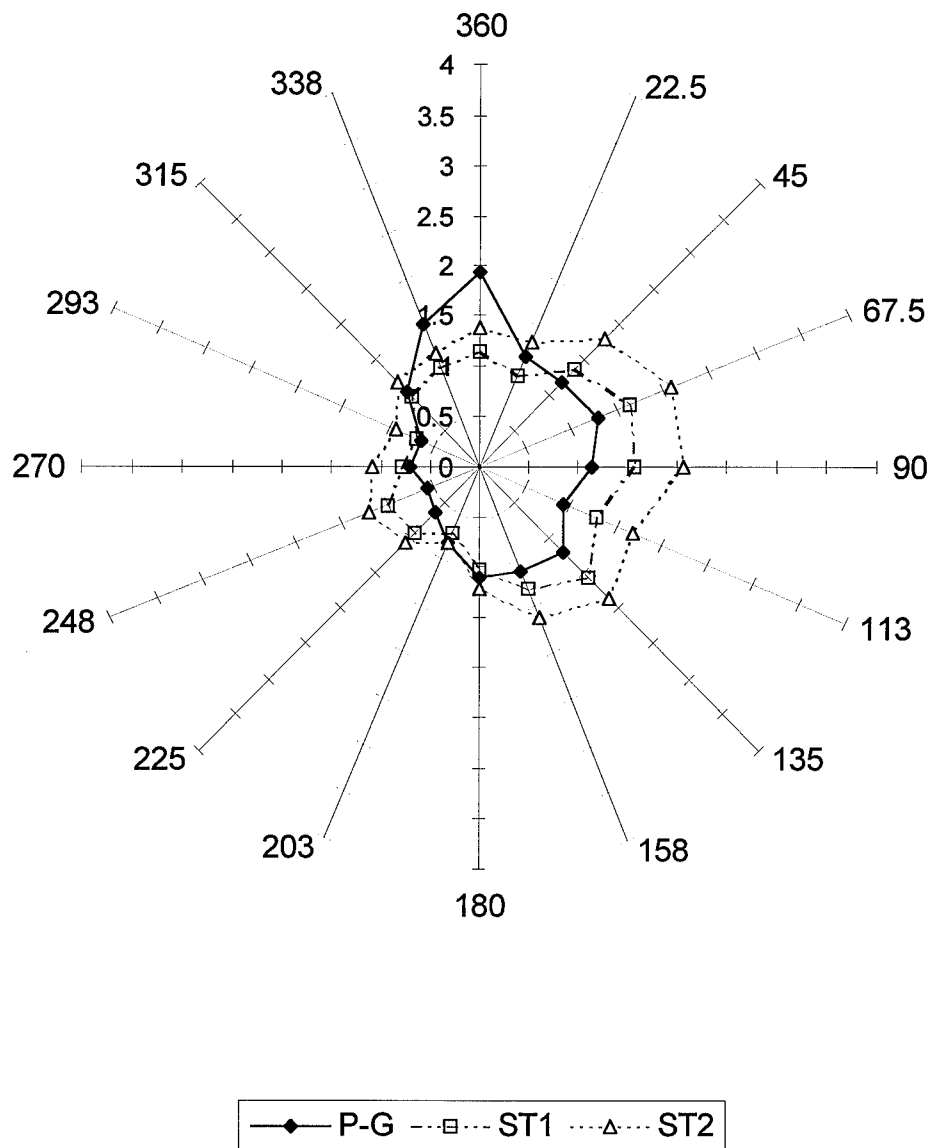


Figure 4.11 Average Period Concentrations For Site 4 10 Meter Data

**Average Period Concentration Ratio For Site 4
Elevated Release**

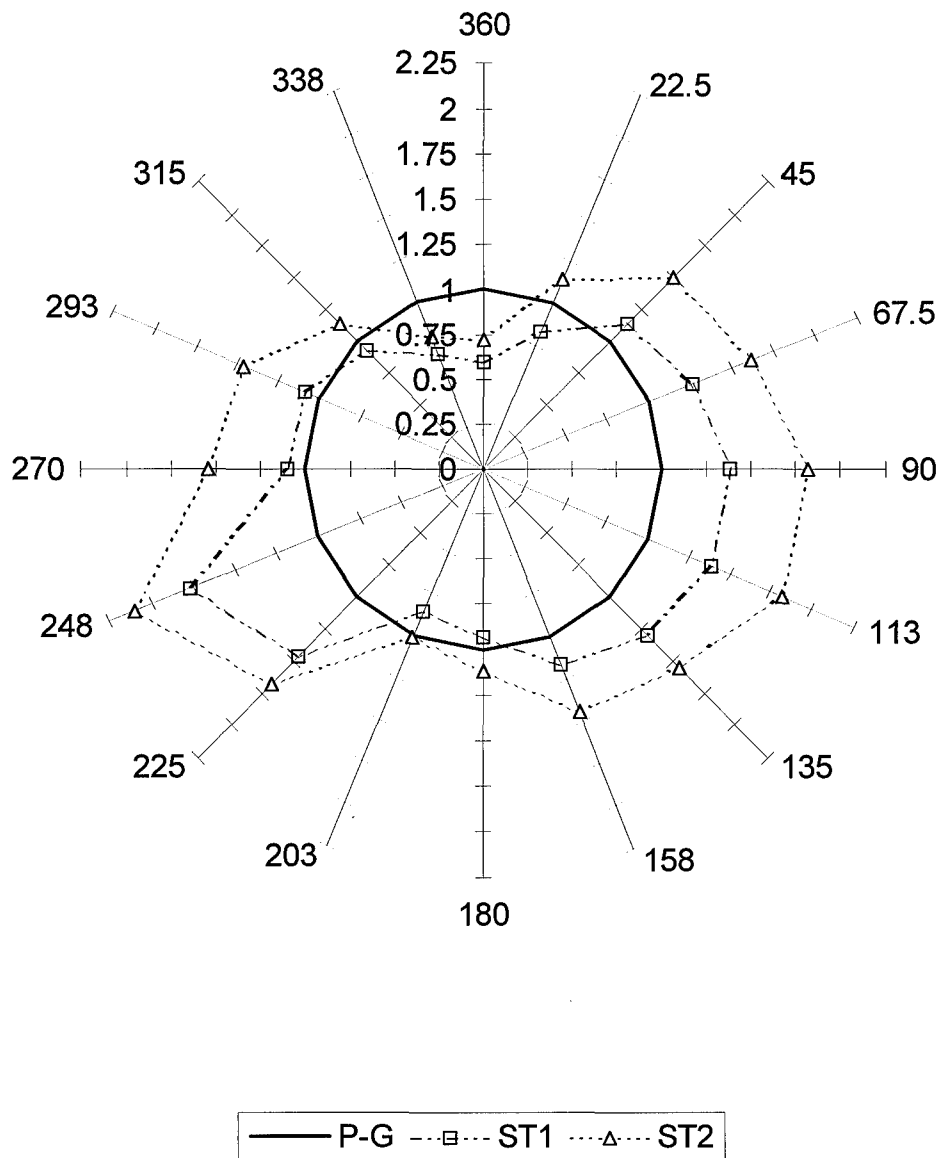


Figure 4.12 Average Period Concentration Ratio For Site 4 10 Meter Data

4.2. *1 Meter Site Parameters*

4.2.1. Wind Data. The 1 meter wind data show the effects of the ground vegetation cover. Figure 4.13 is the frequency distribution of average wind directions for all three sites at the 1 meter level which show that the north-south winds are dominant at all of the sites. This distribution is similar to the 10 meter data, but the effects of the clearings in site 5 are even more pronounced. Sites 2 and 4 are almost replicas of the 10 meter data. The distribution of average wind directions normalized to site 2 as shown in Figure 4.14 are again almost identical to the 10 meter data with the exception of site 5. The disparity in winds from the north at site 5 compared to sites 2 and 4 are accentuated in this view.

The average 1 meter hourly wind speeds are shown in Figure 4.15. The sites should have similar wind speed characteristics because the surface vegetation slows the wind. Sites 2 and 5 meet these expectations, but site 4 has higher wind speeds. A re-examination of site 4 revealed that the access road into the site formed an open channel in the 1.5 meter high prairie grass that allowed the wind unhindered access to the 1 meter sensors, resulting in the higher values.

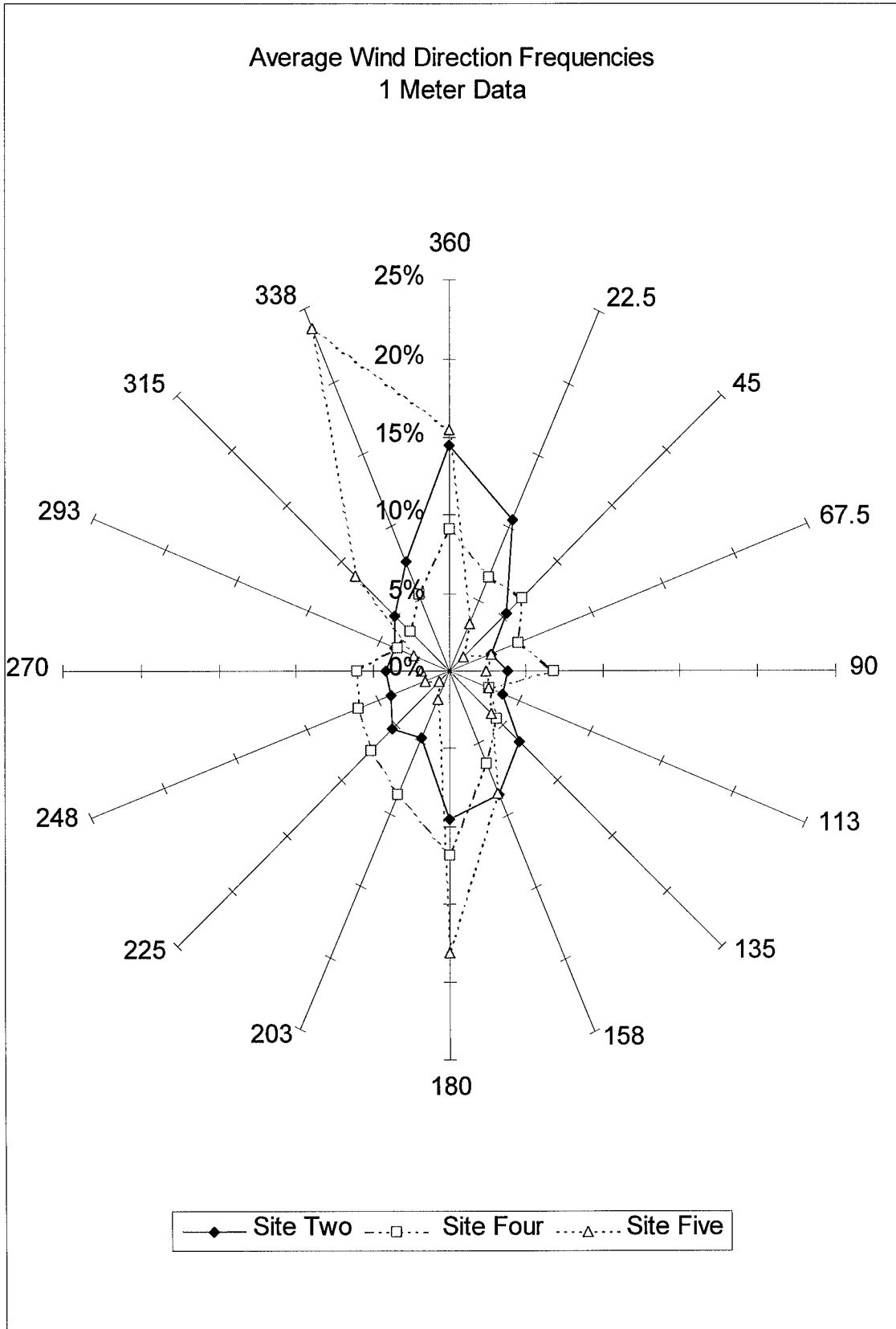


Figure 4.13 Average Wind Direction Frequencies 1 Meter Data

**Normalized Average Wind Direction Frequencies
1 Meter Data**

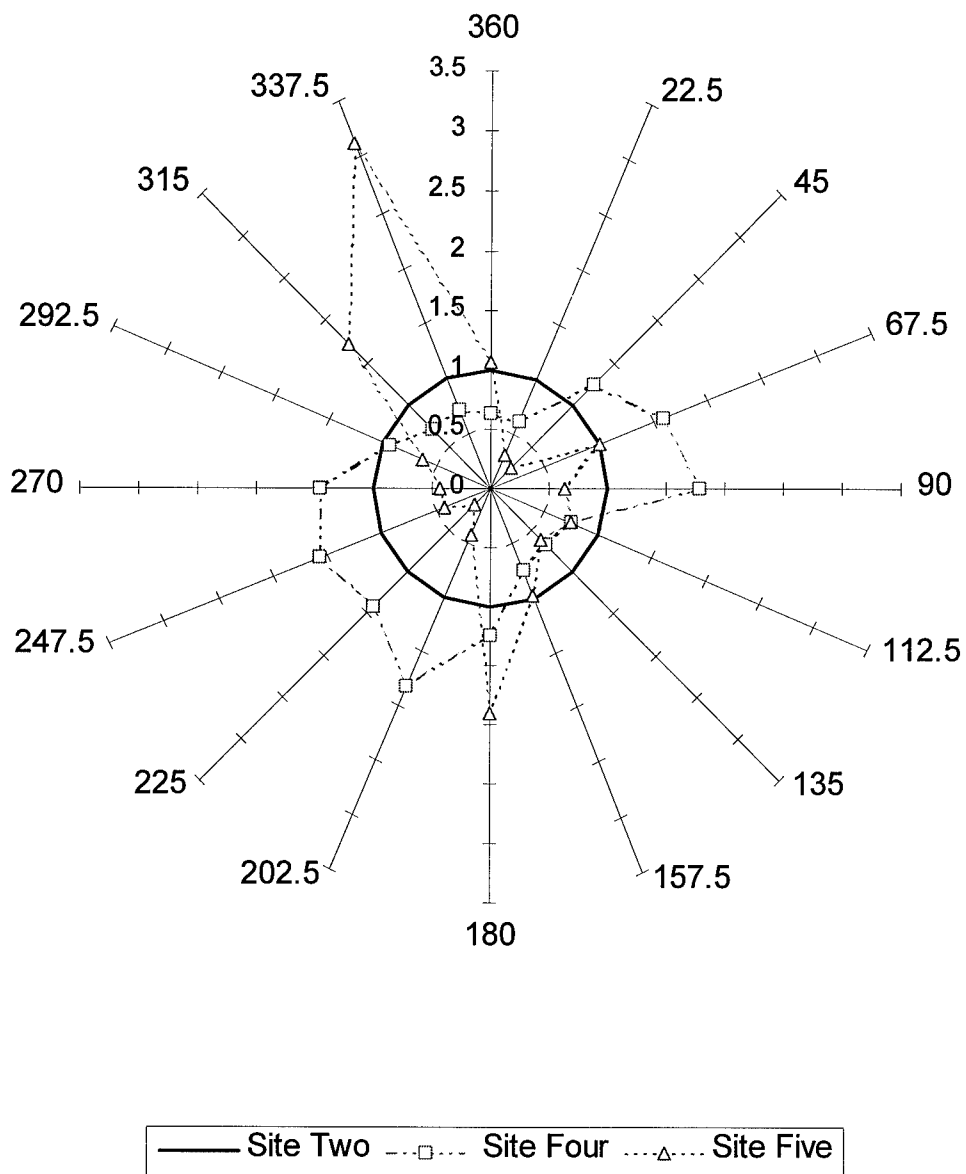


Figure 4.14 Normalized Average Wind Direction Frequencies 1 Meter Data

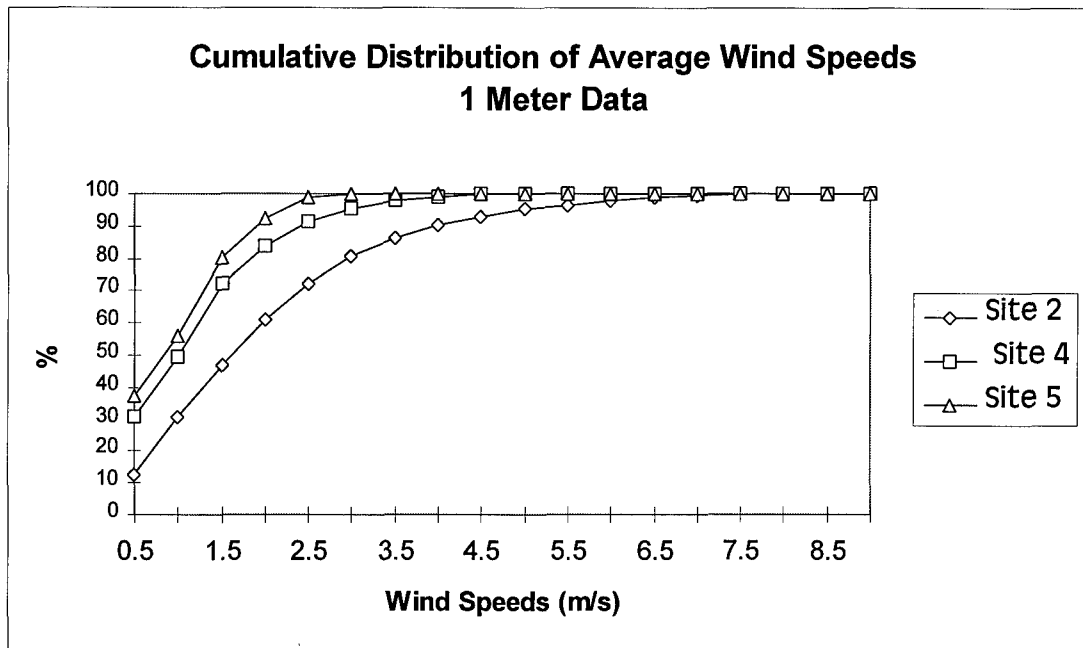


Figure 4.15 Average Wind Speed Distribution For 1 Meter Data

4.2.2. Stability Classification Distribution. The 1 meter distribution of stability levels as determined by the Pasquill-Gifford method and the two σ_θ schemes is presented in Figures 4.16 to 4.18. The 1 meter data shows that the distribution of the stability conditions are more skewed toward the extremely stable and unstable conditions than those of the 10 meter. This result is expected as neutral and near-neutral conditions would occur very infrequently due to the surrounding vegetation slowing the wind, which also introduces mechanical turbulence. When the wind is strong enough to penetrate the vegetative cover, small eddies that compose mechanical turbulence are dominant, leading to the strongly unstable condition for the σ_θ methods. The Pasquill-Gifford method reports the strongly unstable condition for this situation because the wind is slowed as it penetrates the vegetative cover. Site 2 has less of a vegetative cover than the other two sites and has a more even distribution of stability conditions. The difference in the σ_θ

methods from the Pasquill-Gifford method can be explained by the introduction of mechanical turbulence when the wind is light. The Pasquill-Gifford method shows these occurrences as the stable condition F while the σ_0 methods can sense the induced turbulence due to the vegetation and would favor neutral or near-neutral conditions.

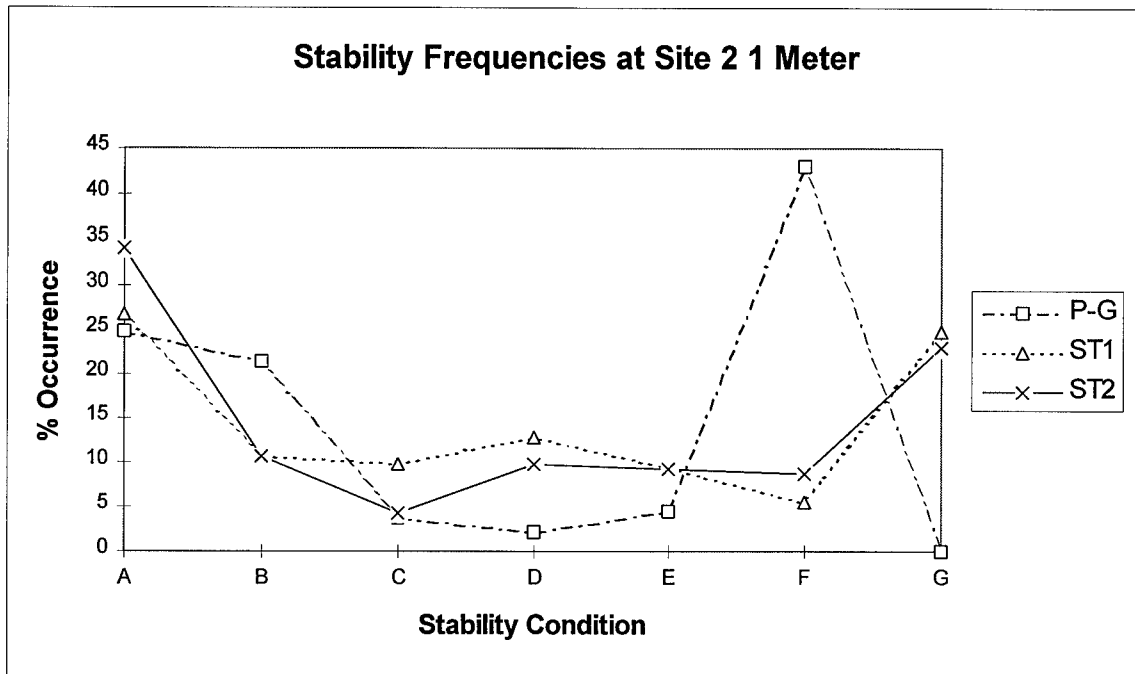


Figure 4.16 Site 2 1 Meter Stability Distribution

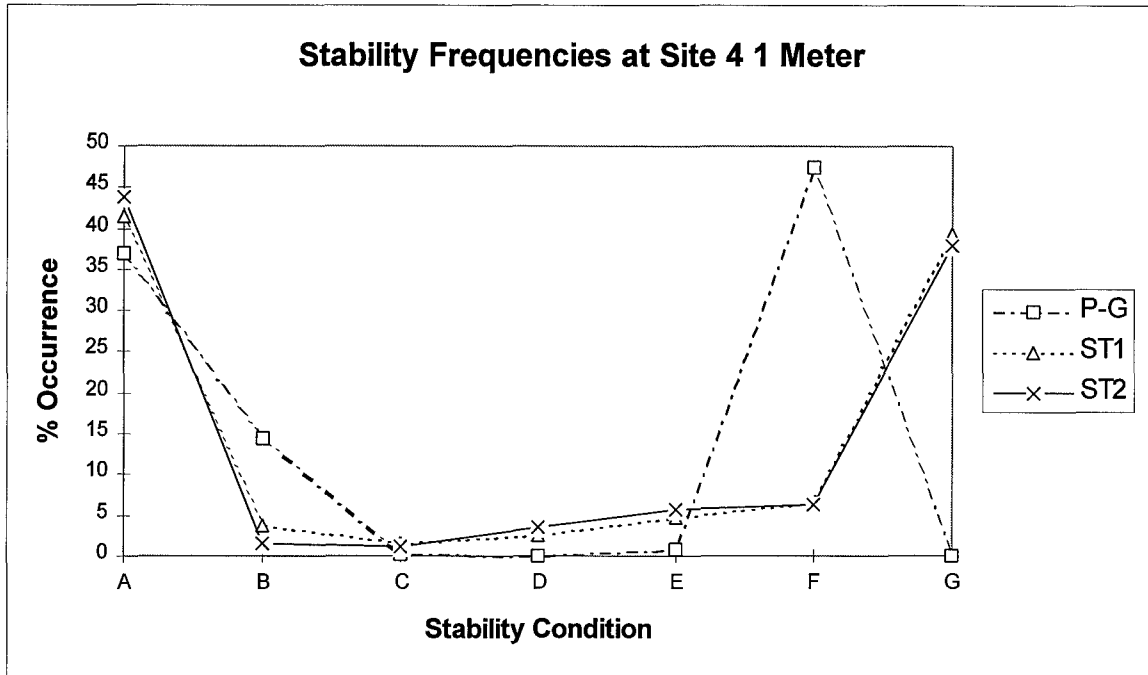


Figure 4.17 Site 4 1 Meter Stability Distribution

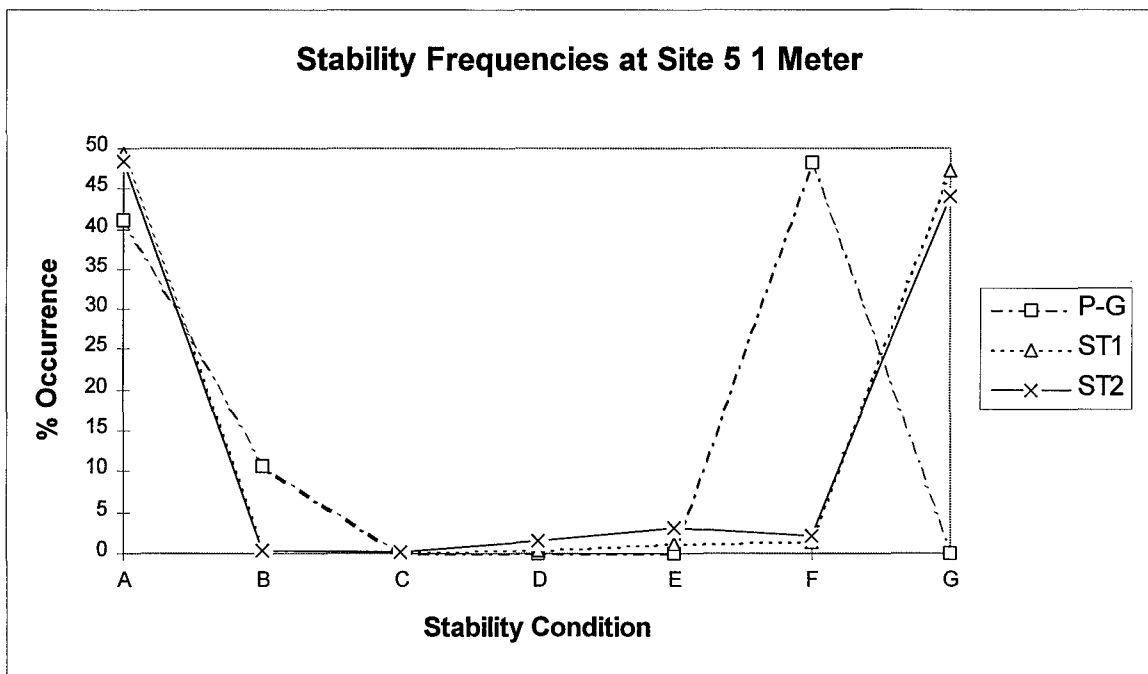


Figure 4.18 Site 5 1 Meter Stability Distribution

4.2.3. ISCST Output. The ground level release case shows that the maximum concentrations are more dependent upon wind direction because of the increased instability at the lower elevations due to the surrounding vegetation in all directions. For

the ground release case, stable conditions have smaller dispersive forces that keep the plume intact that lead to a higher ground level concentration. The greater the dispersive forces, hence the more unstable the atmosphere, lead to lower ground level concentrations as the plume is scattered.

All method are in rough agreement with the two σ_θ methods matching the Pasquill-Gifford method. For site 2 in Figure 4.19, the two maximum concentration spikes lie opposite the prevailing wind conditions. The most common stability condition for the prevailing north-south winds is the strongly stable condition F, leading to the maximum concentrations. Figure 4.20 shows the concentrations of the two σ_θ methods normalized to the concentration determined by the Pasquill-Gifford method. General agreement is shown, but the over-prediction by the Pasquill-Gifford method is probably due to over-reporting of the stable condition F due to method's inability to sense mechanical turbulence.

For site 5's 1 meter run (Figure 4.21), the effect of the prevailing wind condition is most pronounced. With the average wind direction either from north-northwest or from the south, the maximum concentrations are aligned in the exact opposite compass direction without deviation. With a large number of the stable conditions F and G in all directions, the concentration profile is a function of the prevailing wind conditions. From Figure 4.22, the σ_θ methods yield similar concentration profiles and under-predict Pasquill-Gifford. Again, the Pasquill-Gifford method is not effected by the mechanical turbulence introduced by the surrounding vegetation and reports more stable conditions

**Average Period Concentrations For Site 2
Ground Release**

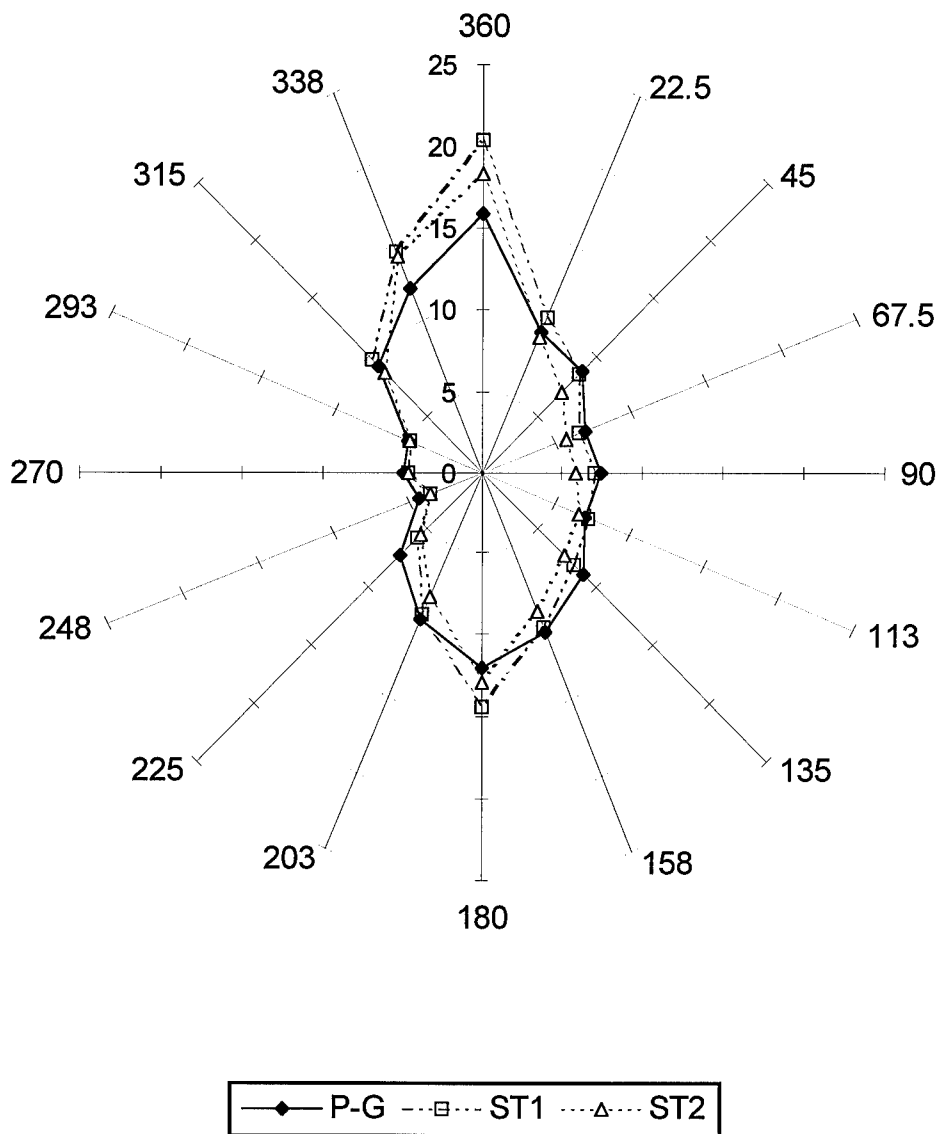


Figure 4.19 Average Period Concentrations For Site 2 1 Meter Data

**Normalized Average Period Concentrations For Site 2
Ground Release**

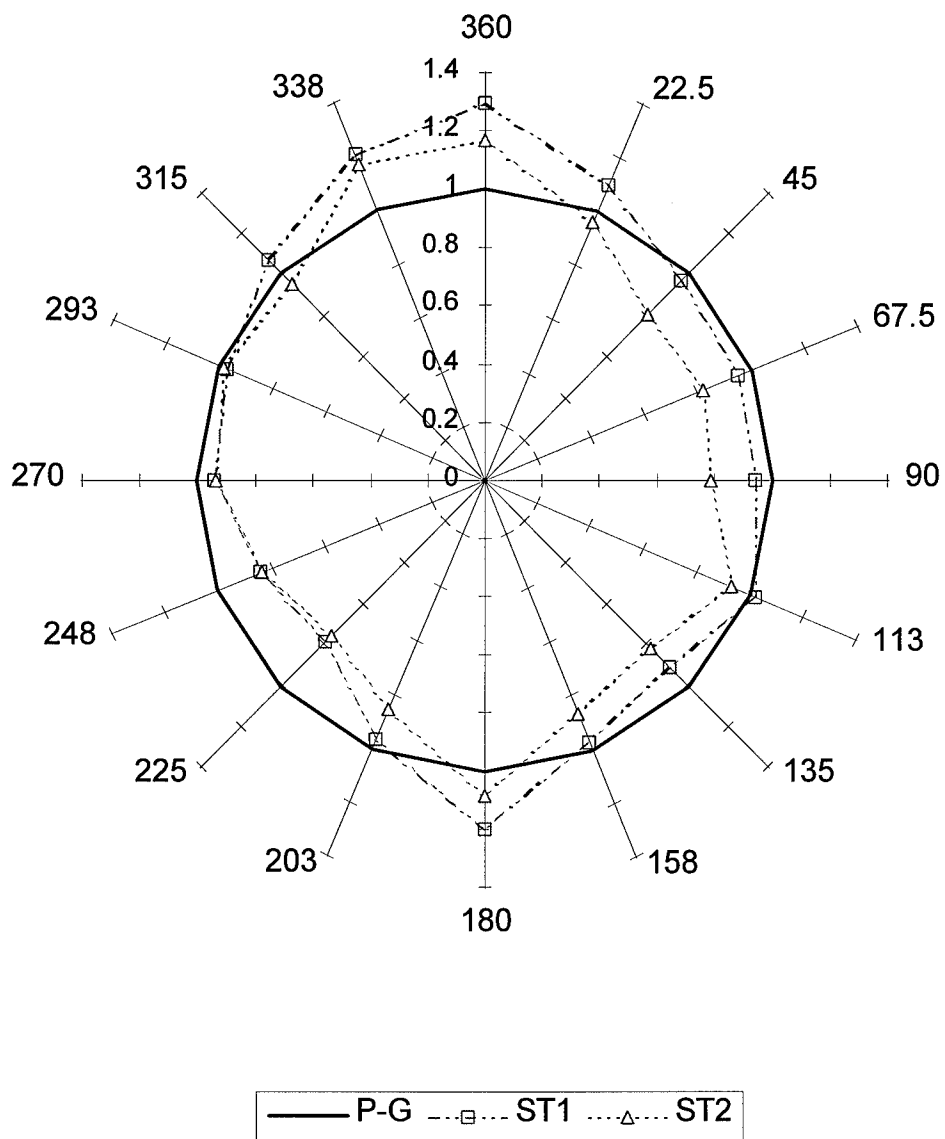


Figure 4.20 Average Period Concentration Ratios For Site 2 1 Meter Data

**Average Period Concentrations For Site 5
Ground Release**

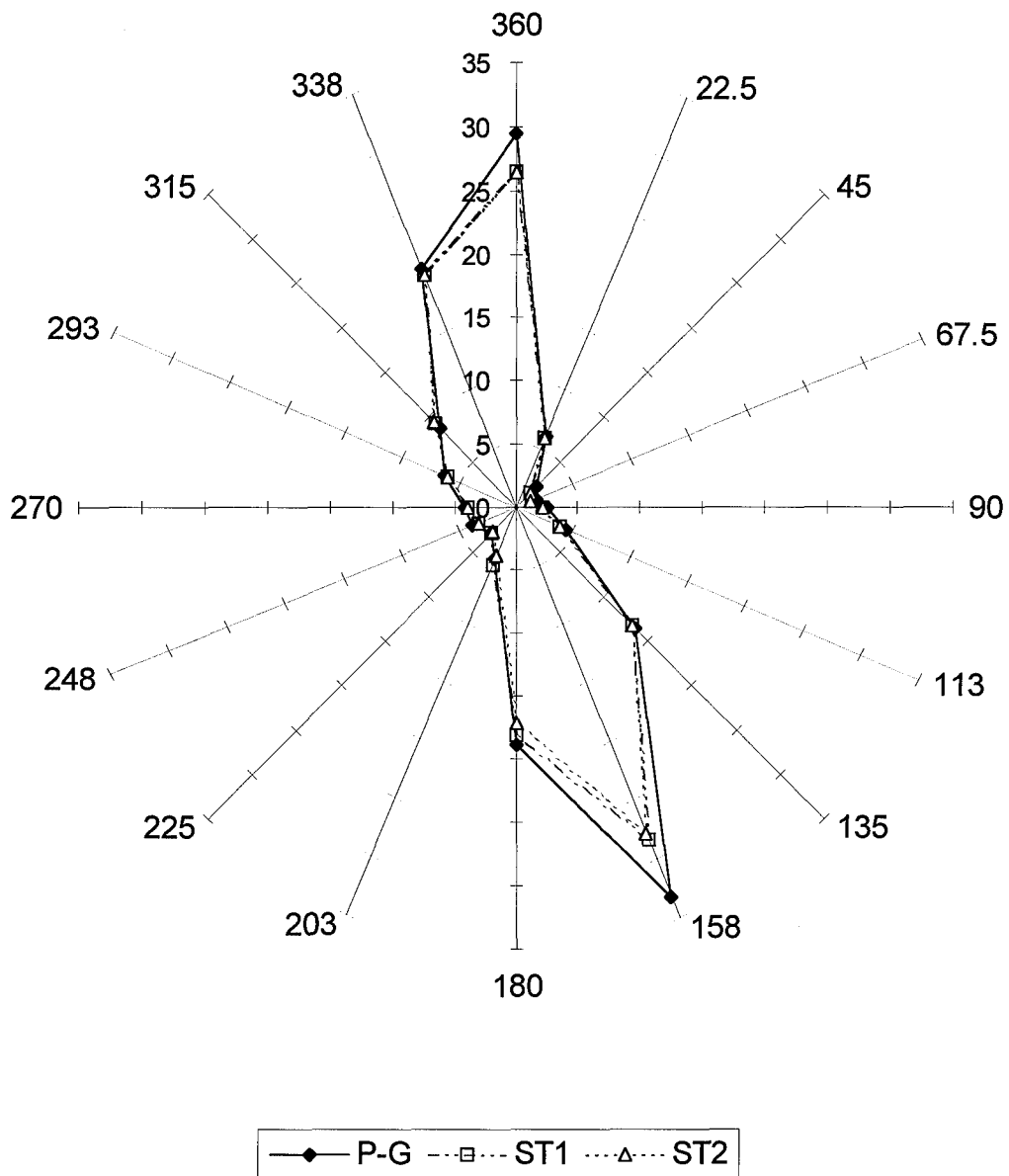


Figure 4.21 Average Period Concentrations For Site 5 1 Meter Data

**Average Period Concentration Ratios For Site 5
Ground Release**

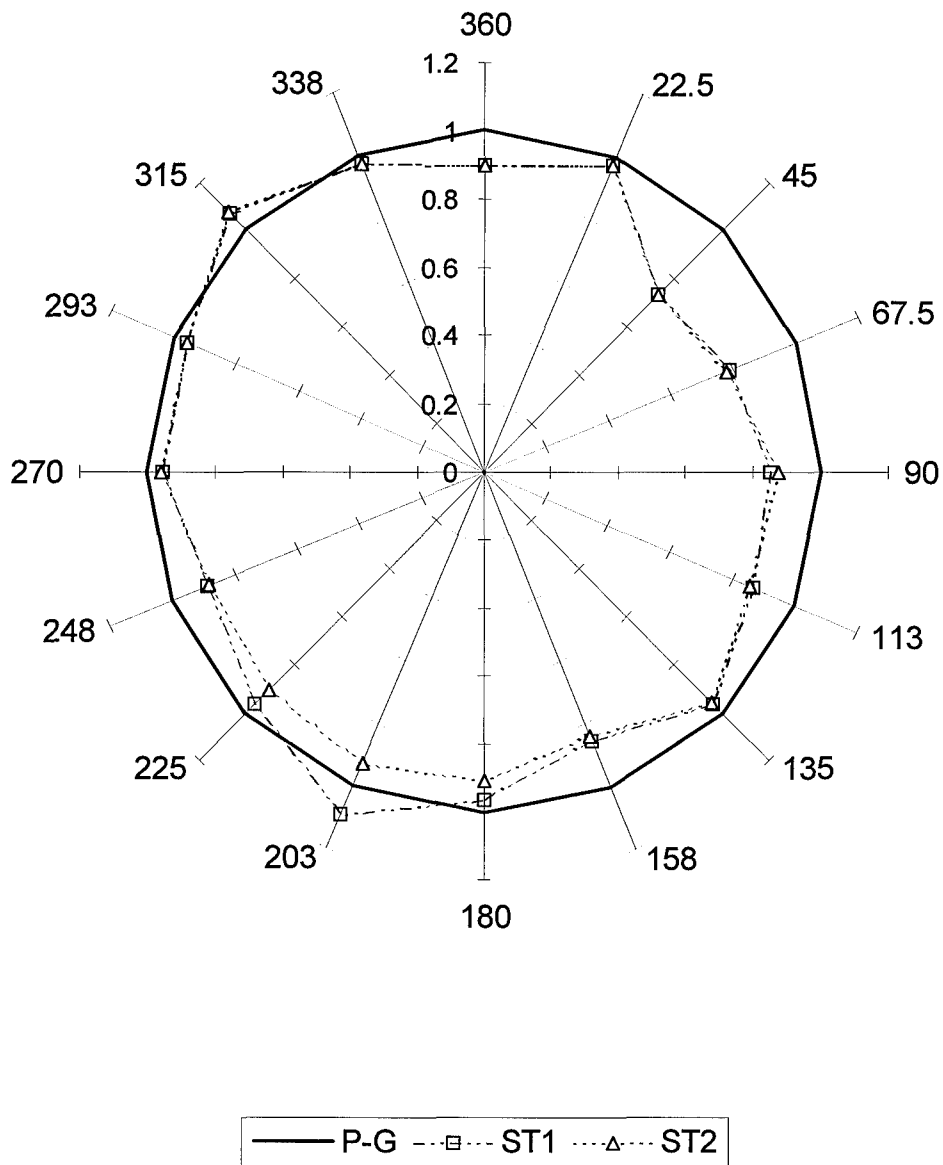


Figure 4.22 Average Period Concentration Ratios For Site 5 1 Meter Data

than are actually present. These more stable conditions lead to the error of higher concentrations in the model's output.

For site 4, the maximum concentrations are again opposite of the prevailing wind direction as shown in Figure 4.23. From due east is a small spike in frequency of wind direction for site 4 from Figure 4.13 which is reflected as a corresponding maximum on the concentration curves to due west. The spike corresponds to the maintenance access road to the site, showing the effects of a small clearing in a prairie. All methods reflect the small clearing to the east with some frequently occurring very unstable conditions from the project data. From Figure 4.24, the σ_θ methods again under-predict Pasquill-Gifford due to Pasquill-Gifford's inability to detect mechanical turbulence introduced by the vegetative cover, leading to a larger number of stable conditions. These stable conditions again lead to higher concentrations.

4.3. *Comparison of Sites*

Since site 2 is a relatively smooth site without obstructions, it will act as the reference site in comparison to 4 and 5 to determine the effect of the vegetation on the prevailing stability conditions and average concentrations. The concentrations at sites 4 and 5 will be normalized to those at site 2 for the derived σ_θ methods (ST1). Figure 4.25 is a comparison of the stability conditions using the Pasquill-Gifford method. Sites 4 and 5 show similar profiles for the Pasquill-Gifford method with a greater occurrence of the very unstable condition A when compared to site 2 with site 5 having the greatest

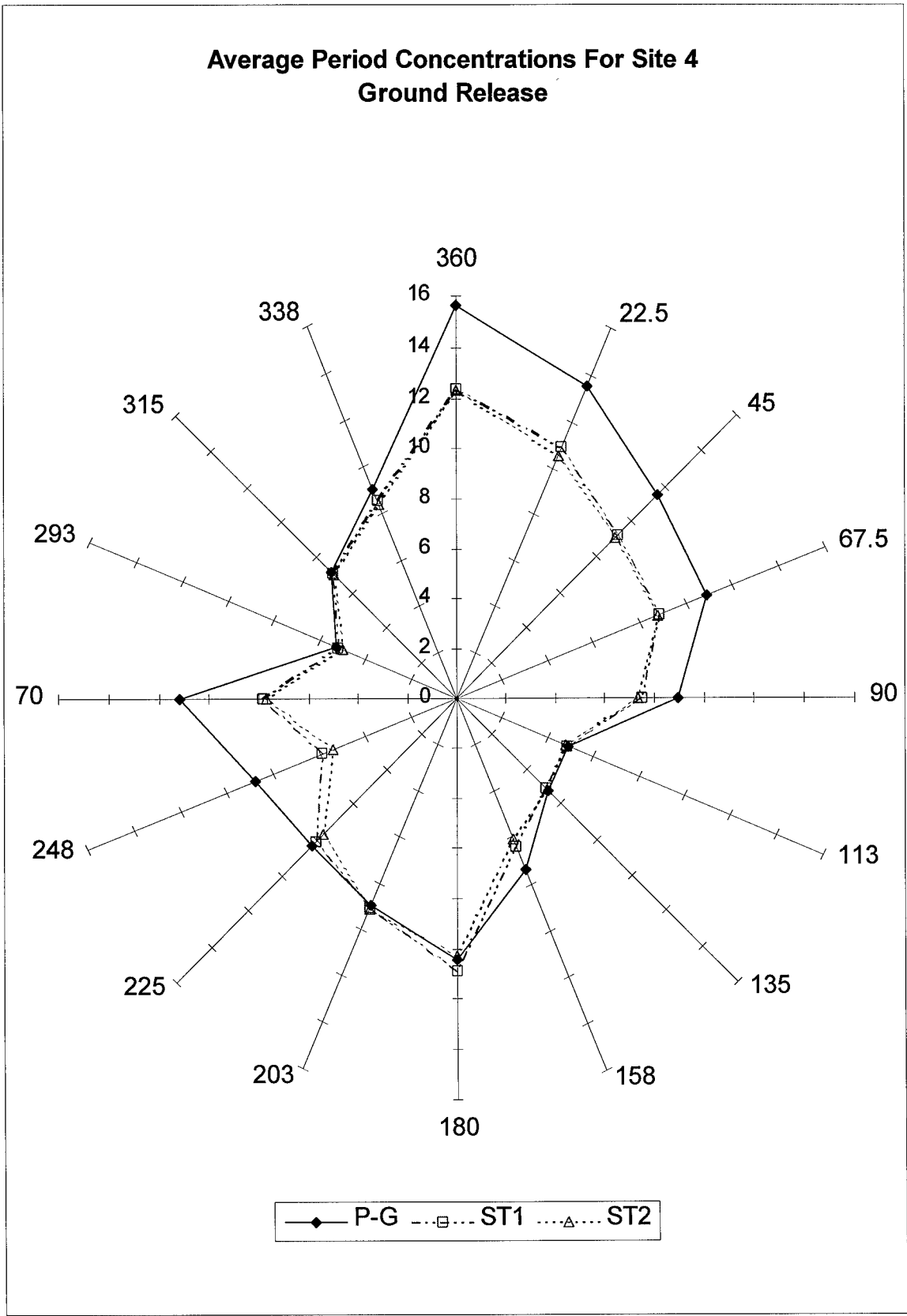


Figure 4.23 Average Period Concentrations For Site 4 1 Meter Data

**Average Period Concentrations Ratios
For Site 4
Ground Release**

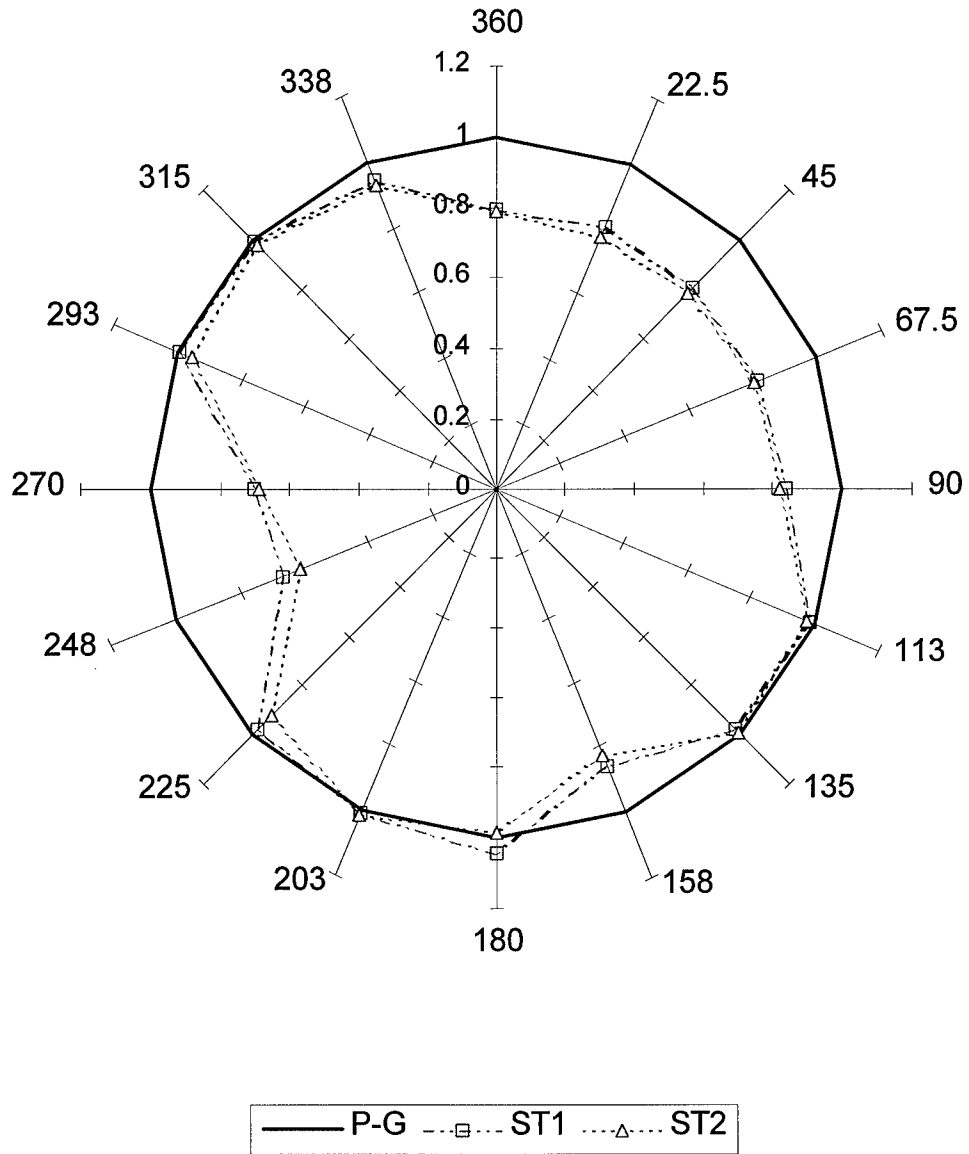


Figure 4.24 Average Period Concentration Ratios For Site 4 1 Meter Data

frequency occurrence. This result is expected as the slower wind speeds experienced at sites 4 and 5 due to the vegetation and the solar insolation values for the site will drive the conditions at 4 and 5 towards greater instability. Higher wind speeds at site 2 will yield a greater frequency of moderately unstable and neutral conditions.

Figure 4.26 is a comparison of the stability conditions using the derived σ_θ method (ST1). The profiles of the sites are comparable to the Pasquill-Gifford method, but there is disagreement in the values of the percent occurrence and at the ends of the stability spectrum (conditions A and G). The moderate and neutral conditions in the σ_θ method at site 2 occur twice as often when compare to the Pasquill-Gifford method. In addition, the σ_θ method is showing greater disparity in the sites at the very unstable condition A due to the mechanical turbulence introduced by the increasing amounts of vegetation from site 2 to site 4 to site 5. There is a 5%-7% increase in the occurrence of condition A at sites 4 and 5 and a 10% decrease in condition B in the σ_θ method when compared to same sites using the Pasquill-Gifford method. The difference in condition B at site 5 are the most illuminating when comparing the two methods as the Pasquill-Gifford method shows an 11% occurrence of condition B while the σ_θ method shows increased turbulence at site 5 being reflected as a greater frequency of condition A and have almost zero occurrences of condition B. This difference reflects the superior ability of the σ_θ method to detect the induced mechanical turbulence from the vegetative canopy over the Pasquill-Gifford method.

Figure 4.27 shows the average concentration ratio for the elevated case. Site 5's concentration profile is far above that of site 2, showing the effects of the increased

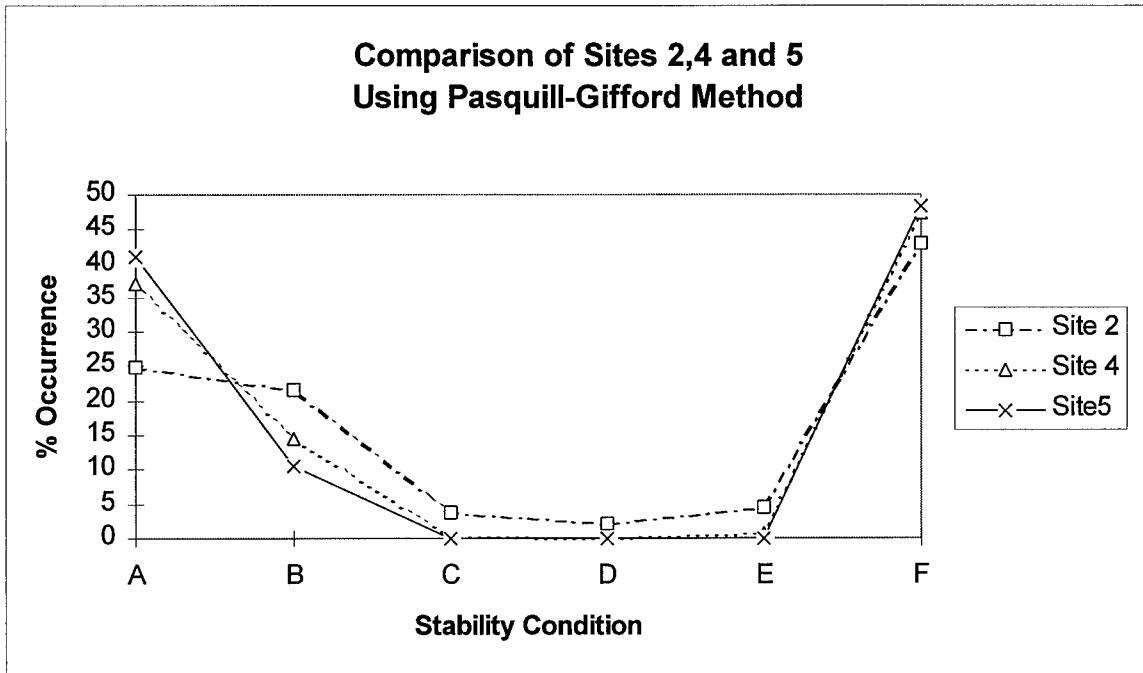


Figure 4.25 Comparison of Sites Using Pasquill-Gifford Method 10 Meter Data

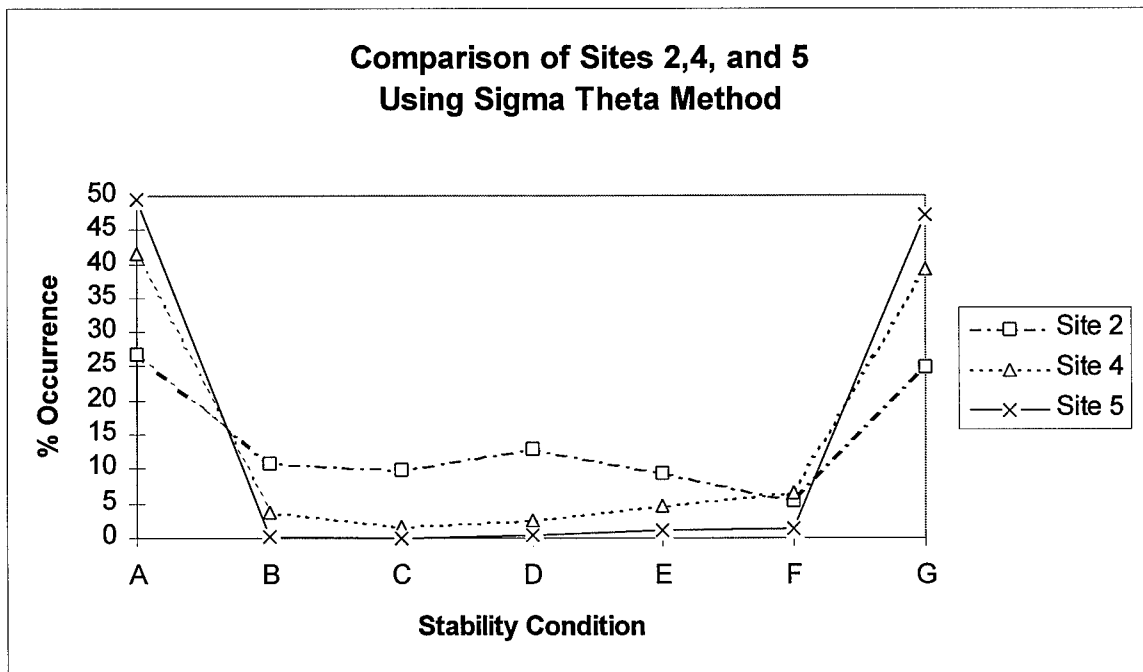
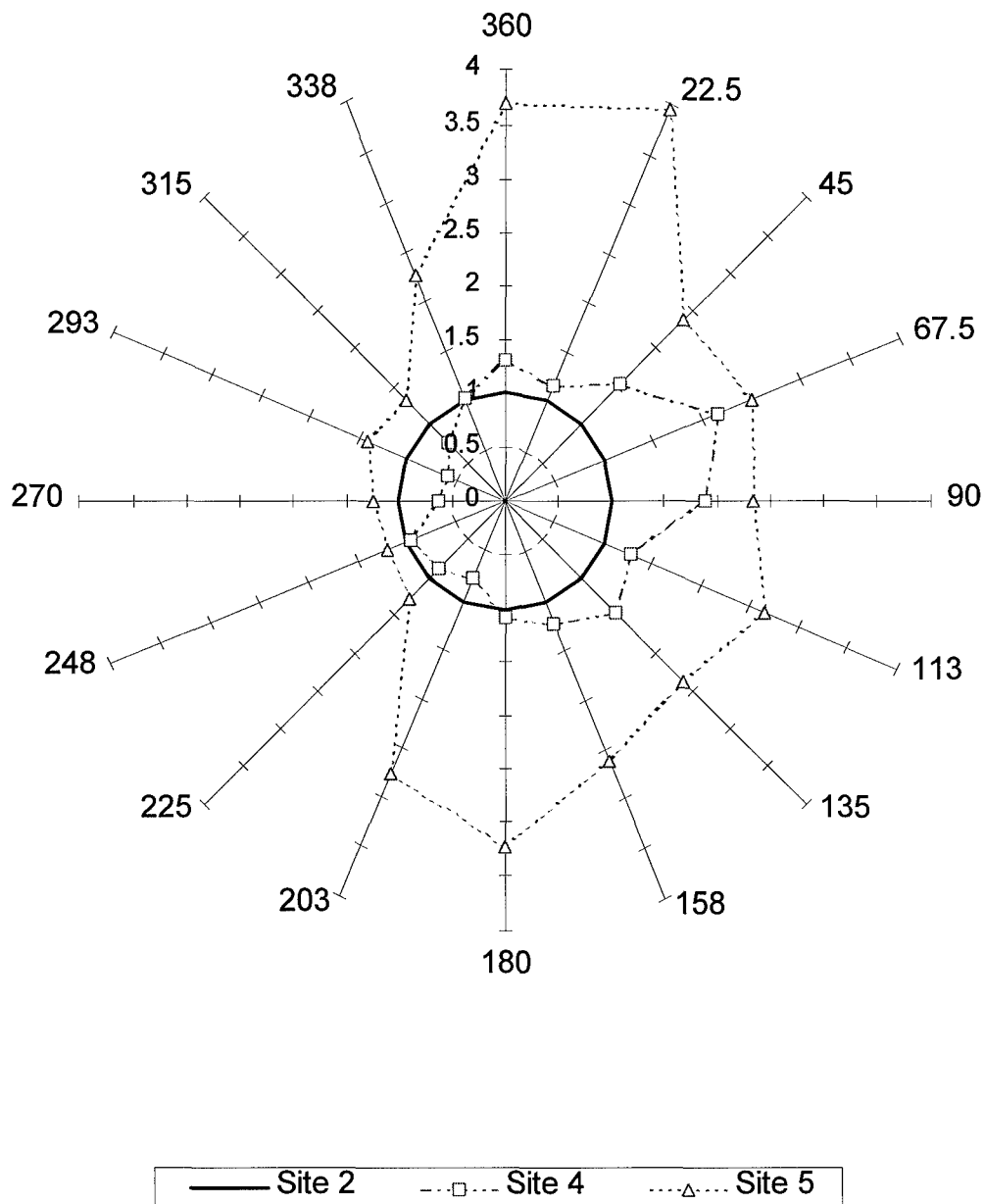


Figure 4.26 Comparison of Sites Using σ_θ Method 10 Meter Data

turbulence introduced by the vegetation. Since there is an elevated plume, the more turbulence in the air, the greater the plume will disperse, causing a higher concentration on the ground. Site 4 also exhibits a higher concentration on the eastern side, but Figure

**Average Period Concentration Ratio
For Sites 2, 4, and 5
Elevated Release**



4.27 Average Period Concentration Ratio For All Sites 10 Meter Data

**Average Period Concentration Ratio
For Sites 2, 4, and 5
Ground Release**

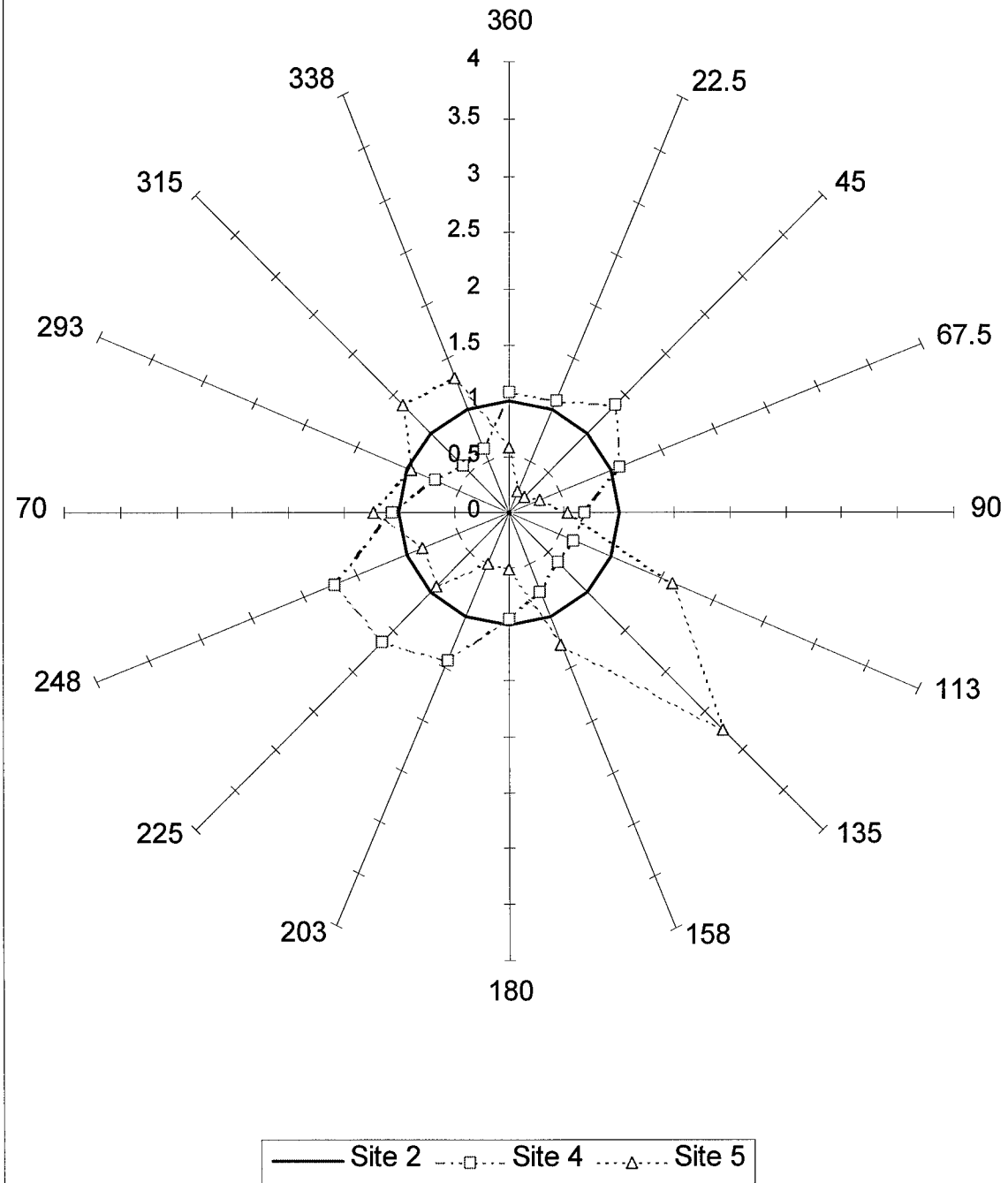


Figure 4.28 Average Concentration Ratio For All Sites 1 Meter Data

curiously is lower than site 2 on the western side. The eastern concentration can be attributed to turbulence introduced to the airstream as it flows over the bog, but the lower western concentration can only be linked to wind frequencies as site 2 has a higher incidence of winds from 135° than does site 4.

The ground level comparison of the sites is at Figure 4.28. The north-south orientation of the concentration contours is similar to all three sites. However, the profile for site 5 is severely skewed due to the distribution at site 5 of the concentration contours. The maximums at site 5 were orientated directly against the prevailing winds in a north-south orientation and had very small average concentrations in east-west directions. Site 4 has a greater frequency of winds from the southwest and northeast and a higher degree of turbulent flow from the bog, giving site 4's profile a distinct east-west characteristic.

4.4. Comparison To Previous Experimentation

The results of this project are comparable to the findings of Mitchell (1980) and Draxler (1987) in their studies of various stability schemes. Although Mitchell did not test the performance of the stability schemes in forested terrain, his results showed that the modified σ_θ scheme (the Modified Mitchell method used in this study) performed better than the Pasquill-Gifford method, especially for short-term studies. He also found that the modified σ_θ scheme was able to better predict peak sector concentrations, similar to the results of this study.

Draxler (1987) used urban areas in his test and determined that the sigma schemes provided a greater frequency of unstable cases (A through C) and far fewer occurrences of

the stable case (F). His overlying conclusion was that the σ_θ scheme when paired with the Pasquill-Gifford dispersion curves provided as good of results as the Pasquill-Gifford method. For the site that might best match urban terrain, site 4, the stability condition distribution for the σ_θ schemes matches the findings of Draxler. Figure 4.29 shows that the σ_θ schemes have almost half of their distribution in the unstable range (46.3% in the derived method ST1 and 49.7% in the power method ST2) while having less than a third of the readings in the stable categories (32% for ST1 and 32.7% for ST2). In addition, both σ_θ methods have few reportings of the F stability class (5.6% in ST1 and 8% in ST2), matching the findings of Draxler.

Pinker and Holland's (1988) results of finding σ_θ values that were substantially larger in forested areas than those over smoother areas is verified by the values of σ_θ at site 5 when compared to those at site 2. Pinker and Holland found that the σ_θ values at a mildly rough site such as a clearing in a prairie were 50% to 100% greater than that of a smooth site, while values for forested terrain were another 50% greater than that of the mildly rough site. Table 4.3 contrast the σ_θ values at site 2 compared to site 5. With either the derived or the power method of averaging the σ_θ values, the means of the σ_θ distributions are almost 50% larger than at site 5 than those at site 2. This large increase shows the effects of the induced turbulence of the forest canopy on the wind flow as it goes over and through the bog.

TABLE 4.3

COMPARISON OF σ_0 VALUES

METHOD	Site 2		Site 5	
	Derived	Power	Derived	Power
MEAN	28.40	25.60	42.56	44.63
SD	23.22	15.92	20.39	18.64
MINIMUM	2.87	3.65	0.00	0.00
MEDIAN	18.78	19.70	38.14	42.06
MAXIMUM	121.65	102.53	121.85	105.56

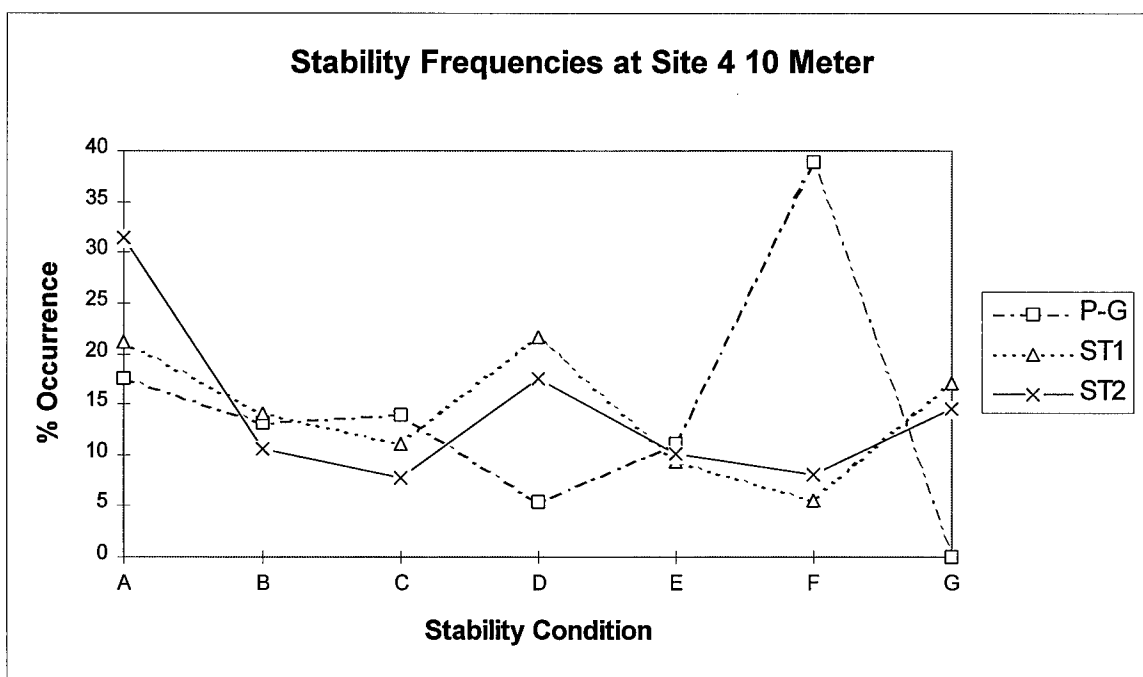


Figure 4.29 Site 4 10 Meter Stability Distribution

V. Conclusions

5.1. *Stability Methods*

The different stability criteria methods had a drastic effect on the outcome of the air pollution model. The reference method-the Pasquill-Gifford method-is the most commonly used means to determine stability criteria, but can it determine that criteria accurately in heavily forested areas? The data from this research would say no based on empirical evidence and at best, would provide a good approximation.

The data conclusively shows that the induced turbulence from upwind obstructions and vegetative canopies alters the stability condition in such a manner that the Pasquill-Gifford method that indirectly measure wind fluctuations underestimate or widely overestimate the amount of turbulence. Comparing the results of the smooth site (site 2) with a complex site like site 5 shows that the data runs using stability methods that indirectly measure turbulence are severely underestimating maximum concentrations when compared to the σ_{θ} methods for elevated plumes.

The effect of choosing a stability criteria method on a modeling effort for a new source in complex terrain can alter the outcome tremendously. Compared to the reference method, concentrations can be off as much as 50% or more by using another indirect measurement method. Using the σ_{θ} methods in determining the stability criteria can ensure that the direct turbulence measurements are reflected in the stability outputs, leading to a more accurate product when running a Gaussian model.

5.2. *Averaging Methods*

Comparing the two σ_θ averaging methods reveals that both methods are comparable in rough terrain, but that the derived method tends to be a better performer in smoother terrain. Although both methods estimate the new variances, it appears that the derived method does a better job of including the variances from the 15 minute to 60 minute transition than does the power method. This conclusion is reached on the basis of the sample standard deviations of the new 60 minute averaged σ_θ 's for both methods and comparing the results to the Pasquill-Gifford method's results. The deviations for the derived method are consistently larger than those of the power method, indicating that the derived method's formulation takes into account more of the variances from the 15 minute averaged data. Although the original variances are gone from the 1 second sensed data, the derived method seems to be the better method for sensing that variance and including it in the 60 minute data.

The effect on the air pollution model is that the two methods gave comparable results with minor exceptions. One of these exceptions is typically in the direction of the maximum average concentration when it lies opposite from the prevailing winds, which occurs at site 5 in the elevated case; the power method always predicted a higher concentration than that of the derived method. I believe the problem lies in the simple averaging of the σ_θ 's for the four 15 minute readings. The stability rose for the two methods at site 5 reveal that the power method has a number of occurrences of the neutral condition from the south, while the derived method has none. This neutral condition would indicate a stronger wind penetrating the bog, with mild turbulence. The derived

method will calculate very little variance as the mean wind direction would remain fairly constant and the wind fluctuations will be small, yielding a very small 60 minute average σ_θ value. The power method, with its averaging of the data, must compute a larger variance, keeping it in the neutral condition while the derived method falls into the slightly stable category. This mismatch of categories would lead to the data file runs with the power method σ_θ s having a greater amount of dispersion occurring in the air.

5.3. *Airborne Dispersion*

For applications in gas or biological warfare, this project seems to enforce prevailing wisdom: head crosswind for the lowest concentrations and stay out of the trees. The greatest factor in determining maximum concentrations even in complex terrain is the prevailing wind directions. It is along that line that the maximum concentrations will occur the furthest from the epicenter of the event. The effect of vegetative canopies is to channel the wind flow in directions that can be different than the prevailing wind conditions from an open site. The complex terrain adds turbulence that will increase the dispersion under the canopy, increasing the concentration. The lowest concentrations would appear to be in the open, far from any vertical obstructions.

5.4. *Recommendations*

The σ_θ methods are the most accurate method of measuring the stability condition of the atmosphere. Instead of an indirect measurement, the direct measurement of the turbulence level offers the advantages of accuracy and ease of use. The EPA's reference

Pasquill-Gifford method falls short even in open terrain in estimating the turbulence because as with any estimation, it is only a guess at the prevailing conditions. With the advent of technology making sensing equipment more affordable and self-contained, the excuses for not using information gathered from the site of interest are waning.

The difference in the time averaging methods are slight, but I feel the derived method of averaging the data offers the advantages of retaining a feel for the variances of the originally sensed data. This inclusion of the variances of the original data is important to the output of an dispersion model. More research into this area on a longer time scale using the future bog data can compare long term trends each method, instead of the short 83 day period used in this research.

Areas for further study would be to verify the results of this project. The release of a tracer gas with sensing equipment placed within and around the bog in a number of different atmospheric conditions would lead to a better understanding of the effects of vegetative canopies on airborne dispersion. In addition, a smoke release with time-lapse photography could plot the possible channel flow within the bog.

Appendix A: ISCST Files

INPUT FILE

** This input runstream file corresponds to the example in Volume I, Section 2,
** of the ISC2 User's Guide, except that the ME DAYRANGE keyword has been
** added to limit processing to only the first ten days of the year (to reduce
** execution time), and the meteorological data are read from an ASCII file
** that was generated by the BINTOASC utility program. Additional output file
** options have also been included to illustrate their usage. To run the
** example, type:
**
** ISCST2 TEST-ST.INP outfil.nam
**
** The results for this example problem are provided in file TEST-ST.OUT.
**
** The EVENTEXP.INP file generated for the ISCEV2 model by running this example
** is the same as the example problem provided for that model: TEST-EV.INP.

CO STARTING

```
TITLEONE A Simple Example Problem for the ISCST2 Model
MODELOPT DFAULT RURAL CONC
AVERTIME 3 24 PERIOD
POLLUTID SO2
RUNORNOT RUN
EVENTFIL EVENTEXP.INP
ERRORFIL ERRORS.OUT
```

CO FINISHED

SO STARTING

```
LOCATION STACK1 POINT 0.0 0.0 0.0
** Point Source   QS  HS  TS  VS  DS
** Parameters:   ---- ---- ---- ---- ---
SRCPARAM STACK1 10.0 0.0 325. 1 5
SRCGROUP ALL
```

SO FINISHED

RE STARTING

```
GRIDPOLR POL1 STA
POL1 ORIG 0.0 0.0
POL1 DIST 500.
POL1 GDIR 16 22.5 22.5
POL1 END
```

RE FINISHED

ME STARTING

INPUTFIL stg55.OUT
ANEMHGHT 10
SURFDATA 12345 1995 Dayton
UAIRDATA 12345 1995 Dayton
DAYRANGE 105-189
wdrotate 180

ME FINISHED

OU STARTING

RECTABLE ALLAVE FIRST-SECOND
MAXTABLE ALLAVE 50
MAXIFILE 3 ALL 30.0 g55.FIL 25
MAXIFILE 24 ALL 10.0 g55.FIL 25

** The following card was changed to use the PLOT format instead of UNIFORM.

POSTFILE 24 ALL PLOT g2455.FIL 20
POSTFILE PERIOD ALL PLOT gper55.FIL 21

** Note that the following two input cards generate PLOTFILES with the file
** unit dynamically allocated by the ISCST2 program. When porting the model
** to another computer system, the user may need to specify the file units
** as is done on the previous four input cards.

** PLOTFILE 3 ALL 2ND PLT03ALL.FIL
** PLOTFILE 24 ALL 2ND PLT24ALL.FIL

OU FINISHED

OUTPUT FILE

** This input runstream file corresponds to the example in Volume I, Section 2,
** of the ISC2 User's Guide, except that the ME DAYRANGE keyword has been
** added to limit processing to only the first ten days of the year (to reduce
** execution time), and the meteorological data are read from an ASCII file
** that was generated by the BINTOASC utility program. Additional output file
** options have also been included to illustrate their usage. To run the
** example, type:
**
** ISCST2 TEST-ST.INP outfil.nam
**
** The results for this example problem are provided in file TEST-ST.OUT.
**
** The EVENTEXP.INP file generated for the ISCEV2 model by running this example
** is the same as the example problem provided for that model: TEST-EV.INP.

CO STARTING

TITLEONE A Simple Example Problem for the ISCST2 Model
MODELOPT DFAULT RURAL CONC
AVERTIME 3 24 PERIOD
POLLUTID SO2
RUNORNOT RUN
EVENTFIL EVENTEXP.INP
ERRORFIL ERRORS.OUT

CO FINISHED

SO STARTING

LOCATION STACK1 POINT 0.0 0.0 0.0
** Point Source QS HS TS VS DS
** Parameters: ---- ---- ---- ---- ---
SRCPARAM STACK1 10.0 5.0 325. 1 5
SRCGROUP ALL

SO FINISHED

RE STARTING

GRIDPOLR POL1 STA
POL1 ORIG 0.0 0.0
POL1 DIST 500.
POL1 GDIR 36 10. 10.
POL1 END

RE FINISHED

ME STARTING

INPUTFIL st55.OUT

ANEMHGHT 10
SURFDATA 12345 1995 Dayton
UAIRDATA 12345 1995 Dayton
DAYRANGE 105-189
ME FINISHED

OU STARTING

RECTABLE ALLAVE FIRST-SECOND
MAXTABLE ALLAVE 50
MAXIFILE 3 ALL 30.0 M55.FIL 25
MAXIFILE 24 ALL 10.0 M55.FIL 25

** The following card was changed to use the PLOT format instead of UNIFORM.

POSTFILE 24 ALL PLOT P2455.FIL 20
POSTFILE PERIOD ALL PLOT PER55.FIL 21

** Note that the following two input cards generate PLOTFILES with the file
** unit dynamically allocated by the ISCST2 program. When porting the model
** to another computer system, the user may need to specify the file units
** as is done on the previous four input cards.

** PLOTFILE 3 ALL 2ND PLT03ALL.FIL
** PLOTFILE 24 ALL 2ND PLT24ALL.FIL

OU FINISHED

*** SETUP Finishes Successfully ***

*** MODEL SETUP OPTIONS SUMMARY ***

-
**Model Is Setup For Calculation of Average CONCentration Values.

**Model Uses RURAL Dispersion.

**Model Uses Regulatory DEFAULT Options:

1. Final Plume Rise.
2. Stack-tip Downwash.
3. Buoyancy-induced Dispersion.
4. Use Calms Processing Routine.
5. Not Use Missing Data Processing Routine.
6. Default Wind Profile Exponents.
7. Default Vertical Potential Temperature Gradients.
8. "Upper Bound" Values for Supersquat Buildings.
9. No Exponential Decay for RURAL Mode

**Model Assumes Receptors on FLAT Terrain.

**Model Assumes No FLAGPOLE Receptor Heights.

**Model Calculates 2 Short Term Average(s) of: 3-HR 24-HR
and Calculates PERIOD Averages

**This Run Includes: 1 Source(s); 1 Source Group(s); and 36 Receptor(s)

**The Model Assumes A Pollutant Type of: SO2

**Model Set To Continue RUNNING After the Setup Testing.

**Output Options Selected:

Model Outputs Tables of PERIOD Averages by Receptor

Model Outputs Tables of Highest Short Term Values by Receptor (RECTABLE
Keyword)

Model Outputs Tables of Overall Maximum Short Term Values (MAXTABLE
Keyword)

Model Outputs External File(s) of Threshold Violations (MAXIFILE Keyword)

Model Outputs External File(s) of Concurrent Values for Postprocessing
(POSTFILE Keyword)

**NOTE: The Following Flags May Appear Following CONC Values: c for Calm
Hours

m for Missing Hours

b for Both Calm and Missing Hours

**Misc. Inputs: Anem. Hgt. (m) = 10.00 ; Decay Coef. = .0000 ; Rot. Angle =
.0

Emission Units = GRAMS/SEC ; Emission Rate Unit

Factor = .10000E+07

Output Units = MICROGRAMS/M**3

**Input Runstream File: T55.INP ; **Output Print File: 55.OUT

**File Created for Event Model: EVENTEXP.INP

**Detailed Error/Message File: ERRORS.OUT

*** POINT SOURCE DATA ***

STACK	STACK	BUILDING	EMISSION RATE	BASE	STACK	STACK	STACK	STACK	STACK
SOURCE	PART.	(GRAMS/SEC)	X	Y	ELEV.	HEIGHT	TEMP.	EXIT	EXIT
VEL.	DIAMETER	EXISTS	SCALAR	VARY					
ID	CATS.	(METERS)	(METERS)	(METERS)	(METERS)	(DEG.K)			
(M/SEC)	(METERS)		BY						

STACK1	0	.10000E+02	.0	.0	.0	5.00	325.00	1.00	5.00
--------	---	------------	----	----	----	------	--------	------	------

NO

*** SOURCE IDs DEFINING SOURCE GROUPS ***

GROUP ID	SOURCE IDs
----------	------------

ALL STACK1 ,

*** GRIDDED RECEPTOR NETWORK SUMMARY ***

*** NETWORK ID: POL1 ; NETWORK TYPE: GRIDPOLR

*** ORIGIN FOR POLAR NETWORK ***

X-ORIG = .00 ; Y-ORIG = .00 (METERS)

*** DISTANCE RANGES OF NETWORK ***
(METERS)

500.0,

*** DIRECTION RADIALS OF NETWORK ***
(DEGREES)

10.0,	20.0,	30.0,	40.0,	50.0,	60.0,	70.0,	80.0,	90.0,	
100.0,	110.0,	120.0,	130.0,	140.0,	150.0,	160.0,	170.0,	180.0,	190.0,
200.0,	210.0,	220.0,	230.0,	240.0,	250.0,	260.0,	270.0,	280.0,	290.0,
300.0,	310.0,	320.0,	330.0,	340.0,	350.0,	360.0,			

*** METEOROLOGICAL DAYS SELECTED FOR
PROCESSING ***

(1=YES; 0=NO)

```

0000000000 0000000000 0000000000 0000000000 0
0000000000
0000000000 0000000000 0000000000 0000000000 0
0000000000
0000111111 1111111111 1111111111 1111111111 1
1111111111
1111111111 1111111111 1111111111 1111111110 0
0000000000
0000000000 0000000000 0000000000 0000000000 0
0000000000
0000000000 0000000000 0000000000 0000000000 0
0000000000
0000000000 0000000000 0000000000 0000000000 0
0000000000
0000000000 0000000000

```

NOTE: METEOROLOGICAL DATA ACTUALLY PROCESSED WILL ALSO DEPEND ON WHAT IS INCLUDED IN THE DATA FILE.

*** UPPER BOUND OF FIRST THROUGH FIFTH WIND
SPEED CATEGORIES ***

(METERS/SEC)

1.54, 3.09, 5.14, 8.23, 10.80,

*** WIND PROFILE EXPONENTS ***

STABILITY CATEGORY	WIND SPEED CATEGORY					
	1	2	3	4	5	6
A	.70000E-01	.70000E-01	.70000E-01	.70000E-01	.70000E-01	.70000E-
01 .70000E-01						
B	.70000E-01	.70000E-01	.70000E-01	.70000E-01	.70000E-01	.70000E-
01 .70000E-01						
C	.10000E+00	.10000E+00	.10000E+00	.10000E+00	.10000E+00	
.10000E+00	.10000E+00					
D	.15000E+00	.15000E+00	.15000E+00	.15000E+00	.15000E+00	
.15000E+00	.15000E+00					

E	.35000E+00	.35000E+00	.35000E+00	.35000E+00
.35000E+00	.35000E+00			
F	.55000E+00	.55000E+00	.55000E+00	.55000E+00
.55000E+00	.55000E+00			

*** VERTICAL POTENTIAL TEMPERATURE

GRADIENTS ***

(DEGREES KELVIN PER METER)

STABILITY CATEGORY	WIND SPEED CATEGORY					
	1	2	3	4	5	6
A	.00000E+00	.00000E+00	.00000E+00	.00000E+00	.00000E+00	
.00000E+00	.00000E+00					
B	.00000E+00	.00000E+00	.00000E+00	.00000E+00	.00000E+00	
.00000E+00	.00000E+00					
C	.00000E+00	.00000E+00	.00000E+00	.00000E+00	.00000E+00	
.00000E+00	.00000E+00					
D	.00000E+00	.00000E+00	.00000E+00	.00000E+00	.00000E+00	
.00000E+00	.00000E+00					
E	.20000E-01	.20000E-01	.20000E-01	.20000E-01	.20000E-01	.20000E-
01 .20000E-01						
F	.35000E-01	.35000E-01	.35000E-01	.35000E-01	.35000E-01	.35000E-
01 .35000E-01						

*** THE FIRST 24 HOURS OF METEOROLOGICAL DATA ***

FILE: st55.OUT

FORMAT: (4I2,2F9.4,F6.1,I2,2F7.1)

SURFACE STATION NO.: 12345

UPPER AIR STATION NO.:

12345

NAME: DAYTON

NAME: DAYTON

YEAR: 1995

YEAR: 1995

FLOW SPEED TEMP STAB MIXING HEIGHT (M)
 YEAR MONTH DAY HOUR VECTOR (M/S) (K) CLASS RURAL
 URBAN

95	4	15	1	230.3	.62	272.3	7	2000.0	2000.0
95	4	15	2	73.7	.56	272.0	7	2000.0	2000.0
95	4	15	3	309.7	.72	271.6	7	2000.0	2000.0
95	4	15	4	15.0	.47	271.0	7	2000.0	2000.0
95	4	15	5	309.6	.22	270.6	7	2000.0	2000.0
95	4	15	6	15.1	.57	271.0	7	2000.0	2000.0
95	4	15	7	215.9	.44	272.2	7	2000.0	2000.0
95	4	15	8	158.5	.48	274.7	1	2000.0	2000.0
95	4	15	9	205.8	1.45	278.0	1	2000.0	2000.0
95	4	15	10	174.5	1.70	281.0	1	2000.0	2000.0
95	4	15	11	180.6	1.97	284.2	1	2000.0	2000.0
95	4	15	12	81.4	1.55	285.8	1	2000.0	2000.0
95	4	15	13	91.4	1.98	286.6	1	2000.0	2000.0
95	4	15	14	113.6	1.66	287.5	1	2000.0	2000.0
95	4	15	15	125.5	1.55	287.9	1	2000.0	2000.0
95	4	15	16	152.1	1.49	287.5	1	2000.0	2000.0
95	4	15	17	162.0	1.28	287.1	1	2000.0	2000.0
95	4	15	18	180.8	1.14	286.4	1	2000.0	2000.0
95	4	15	19	177.8	1.03	285.5	6	2000.0	2000.0
95	4	15	20	176.3	.68	284.2	7	2000.0	2000.0
95	4	15	21	77.0	.64	283.1	7	2000.0	2000.0
95	4	15	22	91.0	1.19	282.7	7	2000.0	2000.0
95	4	15	23	105.2	.77	282.0	7	2000.0	2000.0
95	4	15	24	108.2	.90	281.8	7	2000.0	2000.0

*** NOTES: STABILITY CLASS 1=A, 2=B, 3=C, 4=D, 5=E AND 6=F.

FLOW VECTOR IS DIRECTION TOWARD WHICH WIND IS BLOWING.

*** THE PERIOD (2040 HRS) AVERAGE CONCENTRATION VALUES FOR
 SOURCE GROUP: ALL

*** INCLUDING SOURCE(S): STACK1 ,

*** NETWORK ID: POL1 ; NETWORK TYPE: GRIDPOLR ***

** CONC OF SO2 IN MICROGRAMS/M**3

DIRECTION | DISTANCE (METERS)
(DEGREES) | 500.00

10.00	9.68414
20.00	9.78436
30.00	6.24141
40.00	4.36907
50.00	3.59315
60.00	3.55024
70.00	3.76840
80.00	4.14043
90.00	4.30486
100.00	4.49706
110.00	4.54119
120.00	4.47210
130.00	4.61762
140.00	4.91125
150.00	6.17435
160.00	7.98528
170.00	10.32082
180.00	14.42706
190.00	14.26879
200.00	11.39001
210.00	8.45498
220.00	6.64706
230.00	5.35373
240.00	5.48405
250.00	5.40086
260.00	4.97943
270.00	5.29027
280.00	6.18142
290.00	6.96474
300.00	7.48988
310.00	7.64942
320.00	7.56477
330.00	8.38793
340.00	8.04995
350.00	8.71851
360.00	8.58760

*** THE 3RD HIGHEST 3-HR AVERAGE CONCENTRATION
VALUES FOR SOURCE GROUP:

** CONC OF SO2 IN MICROGRAMS/M**3

**

DIRECTION | DISTANCE (METERS)
(DEGREES) | 500.00

10.0	302.67810 (95050206)
20.0	328.75030 (95050203)
30.0	171.89810 (95050124)
40.0	135.97560 (95060809)
50.0	131.30540 (95060418)
60.0	120.41340 (95053018)
70.0	103.10310 (95053018)
80.0	156.12380 (95061518)
90.0	179.49930 (95061518)
100.0	146.64240 (95060518)
110.0	149.79900 (95060518)
120.0	124.06670 (95050812)
130.0	118.66360 (95052212)
140.0	112.10380 (95053115)
150.0	109.93680 (95060915)
160.0	205.95770 (95051321)
170.0	148.45180 (95062409)
180.0	305.45780 (95052809)
190.0	233.01570 (95052824)
200.0	466.07860 (95041821)
210.0	291.26410 (95041824)
220.0	216.78940 (95041824)
230.0	120.06560 (95041718)
240.0	144.76970 (95041718)
250.0	199.07410 (95041903)
260.0	138.12150 (95060315)
270.0	141.27030 (95060315)
280.0	140.80040 (95062518)
290.0	125.66400 (95051218)
300.0	113.35310 (95061815)
310.0	161.25650 (95061818)
320.0	170.46640 (95061818)
330.0	129.45050 (95061818)
340.0	136.77130 (95070109)
350.0	138.04370 (95070109)
360.0	119.60100 (95070218)

*** THE 1ST HIGHEST 24-HR AVERAGE CONCENTRATION
VALUES FOR SOURCE GROUP: ALL ***
** CONC OF SO2 IN MICROGRAMS/M**3 **

DIRECTION | DISTANCE (METERS)
(DEGREES) | 500.00

10.0	84.59956 (95050224)
20.0	64.53724 (95050224)
30.0	53.30493 (95060424)
40.0	42.79715 (95060824)
50.0	31.92318 (95060824)
60.0	23.99302 (95060824)
70.0	32.64794 (95050124)
80.0	35.65839 (95050124)
90.0	41.77253 (95060524)
100.0	50.09157 (95060524)
110.0	48.96441 (95052724)
120.0	56.85909 (95052724)
130.0	50.74184 (95052724)
140.0	36.37377 (95053124)
150.0	39.60875 (95050324)
160.0	54.26914 (95051324)
170.0	46.81184 (95051324)
180.0	69.52103 (95052824)
190.0	88.46047 (95052824)
200.0	92.54745 (95041824)
210.0	46.05251 (95041824)
220.0	37.60463 (95070624)
230.0	42.81517 (95060724)
240.0	42.96299 (95060724)
250.0	37.09670 (95063024)
260.0	37.82670 (95051724)
270.0	33.18097 (95051724)
280.0	47.16424 (95051124)
290.0	48.59079 (95051124)
300.0	41.71358 (95042824)
310.0	59.72098 (95061824)
320.0	46.98355 (95061824)
330.0	54.69604 (95070124)
340.0	57.20116 (95070124)
350.0	41.56185 (95070224)
360.0	55.26312 (95070224)

*** THE 2ND HIGHEST 24-HR AVERAGE CONCENTRATION
VALUES FOR SOURCE GROUP: ALL ***
** CONC OF SO2 IN MICROGRAMS/M**3

DIRECTION		DISTANCE (METERS)
(DEGREES)	500.00	

10.0	53.25854 (95061924)
20.0	62.29654 (95042424)
30.0	47.40026 (95060824)
40.0	38.82055 (95060424)
50.0	26.69882 (95052624)
60.0	23.13764 (95062224)
70.0	26.30935 (95062224)
80.0	31.38485 (95062224)
90.0	30.73946 (95062224)
100.0	44.85052 (95050824)
110.0	46.01979 (95050824)
120.0	40.41136 (95042024)
130.0	41.94735 (95042024)
140.0	34.81020 (95052224)
150.0	39.12583 (95053124)
160.0	51.29363 (95050324)
170.0	42.99942 (95050924)
180.0	56.17365 (95050924)
190.0	67.55326 (95060624)
200.0	49.58708 (95062024)
210.0	41.42811 (95070624)
220.0	31.40319 (95060724)
230.0	32.45820 (95052924)
240.0	37.90110 (95063024)
250.0	35.12299 (95041924)
260.0	28.61765 (95063024)
270.0	25.39505 (95060324)
280.0	35.41581 (95041924)
290.0	47.05200 (95052124)
300.0	41.53357 (95061824)
310.0	41.01457 (95050524)
320.0	42.84045 (95061424)
330.0	49.45464 (95061124)
340.0	53.26206 (95061124)
350.0	40.82617 (95061224)
360.0	51.68768 (95061224)

*** THE MAXIMUM 50 3-HR AVERAGE CONCENTRATION
VALUES FOR SOURCE GROUP: ALL ***
INCLUDING SOURCE(S): STACK1 ,

** CONC OF SO2 IN MICROGRAMS/M**3

**

RANK CONC (YYMMDDHH) AT RECEPTOR (XR,YR) OF TYPE RANK
CONC (YYMMDDHH) AT RECEPTOR (XR,YR) OF TYPE

1.	466.07860 (95041821) AT (-171.01, -469.85) GP	26.	150.47180
	(95042406) AT (171.01, 469.85) GP		
2.	328.75030 (95050203) AT (171.01, 469.85) GP	27.	149.79900
	(95060518) AT (469.85, -171.01) GP		
3.	305.45780 (95052809) AT (.00, -500.00) GP	28.	148.45580
	(95062409) AT (171.01, -469.85) GP		
4.	302.67810 (95050206) AT (86.82, 492.40) GP	29.	148.45180
	(95062409) AT (86.82, -492.40) GP		
5.	292.98670 (95050124) AT (171.01, 469.85) GP	30.	148.20790
	(95060412) AT (171.01, 469.85) GP		
6.	291.26410 (95041824) AT (-250.00, -433.01) GP	31.	146.64240
	(95060518) AT (492.40, -86.82) GP		
7.	283.36170 (95051324) AT (.00, -500.00) GP	32.	145.04710
	(95052809) AT (-86.82, -492.40) GP		
8.	233.01570 (95052824) AT (-86.82, -492.40) GP	33.	144.76970
	(95041718) AT (-433.01, -250.00) GP		
9.	227.18590 (95051818) AT (171.01, 469.85) GP	34.	144.60510
	(95062512) AT (-250.00, -433.01) GP		
10.	216.78940 (95041824) AT (-321.39, -383.02) GP	35.	143.51520
	(95062809) AT (86.82, -492.40) GP		
11.	206.41480 (95051903) AT (171.01, 469.85) GP	36.	143.25720
	(95063012) AT (-469.85, -171.01) GP		
12.	205.95770 (95051321) AT (171.01, -469.85) GP	37.	143.12260
	(95050318) AT (171.01, -469.85) GP		
13.	203.24030 (95042403) AT (171.01, 469.85) GP	38.	141.27030
	(95060315) AT (-500.00, .00) GP		
14.	199.07410 (95041903) AT (-469.85, -171.01) GP	39.	140.80040
	(95062518) AT (-492.40, 86.82) GP		
15.	190.49570 (95062009) AT (-86.82, -492.40) GP	40.	139.92420
	(95052515) AT (86.82, 492.40) GP		
16.	179.49930 (95061518) AT (500.00, .00) GP	41.	138.77410
	(95062809) AT (.00, -500.00) GP		
17.	171.89810 (95050124) AT (250.00, 433.01) GP	42.	138.49880
	(95052821) AT (-86.82, -492.40) GP		

18.	170.46640 (95061818) AT (-321.39, 383.02) GP	43.	138.12150
	(95060315) AT (-492.40, -86.82) GP		
19.	161.49840 (95050203) AT (86.82, 492.40) GP	44.	138.04370
	(95070109) AT (-86.82, 492.40) GP		
20.	161.25650 (95061818) AT (-383.02, 321.39) GP	45.	136.77130
	(95070109) AT (-171.01, 469.85) GP		
21.	160.53870 (95062009) AT (.00, -500.00) GP	46.	135.97560
	(95060809) AT (321.39, 383.02) GP		
22.	160.15010 (95041824) AT (-171.01, -469.85) GP	47.	135.08570
	(95051324) AT (86.82, -492.40) GP		
23.	156.12380 (95061518) AT (492.40, 86.82) GP	48.	134.94670
	(95052618) AT (250.00, 433.01) GP		
24.	154.18900 (95051903) AT (86.82, 492.40) GP	49.	134.35980
	(95060412) AT (250.00, 433.01) GP		
25.	151.42860 (95061918) AT (86.82, 492.40) GP	50.	134.26730
	(95050318) AT (86.82, -492.40) GP		

*** RECEPTOR TYPES: GC = GRIDCART

GP = GRIDPOLR

DC = DISCCART

DP = DISCPOLR

BD = BOUNDARY

*** THE MAXIMUM 50 24-HR AVERAGE
 CONCENTRATION VALUES FOR SOURCE GROUP: ALL ***
 INCLUDING SOURCE(S): STACK1 ,

** CONC OF SO2 IN MICROGRAMS/M**3

**

RANK CONC (YYMMDDHH) AT RECEPTOR (XR,YR) OF TYPE RANK
 CONC (YYMMDDHH) AT RECEPTOR (XR,YR) OF TYPE

1.	92.54745 (95041824) AT (-171.01, -469.85) GP	26.	51.92139
	(95050124) AT (171.01, 469.85) GP		
2.	88.46047 (95052824) AT (-86.82, -492.40) GP	27.	51.91235
	(95042624) AT (-86.82, -492.40) GP		
3.	84.59956 (95050224) AT (86.82, 492.40) GP	28.	51.68768
	(95061224) AT (.00, 500.00) GP		
4.	69.52103 (95052824) AT (.00, -500.00) GP	29.	51.29363
	(95050324) AT (171.01, -469.85) GP		
5.	67.55326 (95060624) AT (-86.82, -492.40) GP	30.	50.74184
	(95052724) AT (383.02, -321.39) GP		
6.	64.53724 (95050224) AT (171.01, 469.85) GP	31.	50.70117
	(95061224) AT (86.82, 492.40) GP		
7.	62.88952 (95062824) AT (-86.82, -492.40) GP	32.	50.09157
	(95060524) AT (492.40, -86.82) GP		
8.	62.29654 (95042424) AT (171.01, 469.85) GP	33.	49.87270
	(95051824) AT (171.01, 469.85) GP		
9.	59.72098 (95061824) AT (-383.02, 321.39) GP	34.	49.58708
	(95062024) AT (-171.01, -469.85) GP		
10.	57.20116 (95070124) AT (-171.01, 469.85) GP	35.	49.45464
	(95061124) AT (-250.00, 433.01) GP		
11.	56.85909 (95052724) AT (433.01, -250.00) GP	36.	49.43469
	(95060624) AT (.00, -500.00) GP		
12.	56.17365 (95050924) AT (.00, -500.00) GP	37.	49.16060
	(95070424) AT (-86.82, -492.40) GP		
13.	55.30764 (95062824) AT (.00, -500.00) GP	38.	49.10403
	(95061924) AT (.00, 500.00) GP		
14.	55.26312 (95070224) AT (.00, 500.00) GP	39.	49.08333
	(95052524) AT (171.01, 469.85) GP		
15.	55.13376 (95070424) AT (.00, -500.00) GP	40.	48.96441
	(95052724) AT (469.85, -171.01) GP		
16.	54.89095 (95060424) AT (171.01, 469.85) GP	41.	48.77682
	(95070524) AT (-86.82, -492.40) GP		
17.	54.69604 (95070124) AT (-250.00, 433.01) GP	42.	48.60426
	(95060424) AT (86.82, 492.40) GP		

18.	54.43944 (95062924) AT (.00, -500.00) GP	43.	48.59079
	(95051124) AT (-469.85, 171.01) GP		
19.	54.26914 (95051324) AT (171.01, -469.85) GP	44.	48.49236
	(95052524) AT (86.82, 492.40) GP		
20.	53.53246 (95062924) AT (-86.82, -492.40) GP	45.	47.40026
	(95060824) AT (250.00, 433.01) GP		
21.	53.30493 (95060424) AT (250.00, 433.01) GP	46.	47.16424
	(95051124) AT (-492.40, 86.82) GP		
22.	53.26206 (95061124) AT (-171.01, 469.85) GP	47.	47.08278
	(95070624) AT (-86.82, -492.40) GP		
23.	53.25854 (95061924) AT (86.82, 492.40) GP	48.	47.05200
	(95052124) AT (-469.85, 171.01) GP		
24.	52.91789 (95062024) AT (-86.82, -492.40) GP	49.	47.02991
	(95061424) AT (-250.00, 433.01) GP		
25.	52.12474 (95070224) AT (86.82, 492.40) GP	50.	46.98355
	(95061824) AT (-321.39, 383.02) GP		

*** RECEPTOR TYPES: GC = GRIDCART
 GP = GRIDPOLR
 DC = DISCCART
 DP = DISCPOLR
 BD = BOUNDARY

***THE SUMMARY OF MAXIMUM PERIOD (2040 HRS) RESULTS ***

** CONC OF SO2 IN MICROGRAMS/M**3

**

GROUP ID	AVERAGE CONC	NETWORK RECEPTOR (XR, YR, ZELEV, ZFLAG) OF TYPE GRID-ID
ALL	14.42706	AT (.00, -500.00, .00, .00) GP POL1
	14.26879	AT (-86.82, -492.40, .00, .00) GP POL1
	11.39001	AT (-171.01, -469.85, .00, .00) GP POL1
	10.32082	AT (86.82, -492.40, .00, .00) GP POL1
	9.78436	AT (171.01, 469.85, .00, .00) GP POL1
	9.68414	AT (86.82, 492.40, .00, .00) GP POL1

*** THE SUMMARY OF HIGHEST 3-HR RESULTS ***

** CONC OF SO2 IN MICROGRAMS/M**3

**

GROUP ID	AVERAGE CONC (YYMMDDHH)	NETWORK RECEPTOR (XR, YR, ZELEV, ZFLAG) OF TYPE GRID-ID
ALL	466.07860	ON 95041821: AT (-171.01, -469.85, .00, .00) GP POL1
	292.98670	ON 95050124: AT (171.01, 469.85, .00, .00) GP POL1

*** ISCST2 - VERSION 93109 *** *** A Simple Example Problem for the ISCST2 Model *** 09/15/95

*** ISCST2 - VERSION 93109 *** *** A Simple Example Problem for the ISCST2
Model *** 09/15/95

*** 17:34:36

PAGE 17

*** MODELING OPTIONS USED: CONC RURAL FLAT

DFAULT

*** Message Summary For ISC2 Model Execution ***

----- Summary of Total Messages -----

A Total of 0 Fatal Error Message(s)
A Total of 0 Warning Message(s)
A Total of 1 Informational Message(s)

A Total of 1 Calm Hours Identified

***** FATAL ERROR MESSAGES *****
*** NONE ***

***** WARNING MESSAGES *****
*** NONE ***

*** ISCST2 Finishes Successfully ***

Bibliography

- Cionco, Ronald M. "Modeling Windfields and Surface Layer Wind Profiles Over Complex Terrain and Within Vegetative Canopies" in Forest-Atmosphere Interaction. Bremen, Germany: D. Reidel Publishing Company (1985).
- Cramer, H.E. "A Practical Method For Estimating the Dispersion of Atmospheric Contaminants," in Proceedings of the 1st National Conference on Applied Meteorology. New Orleans, LA: American Meteorology Society (1957).
- Cramer, H.E., et. al. "Engineering Estimates of Atmospheric Dispersal Capacity," Journal of the American Industrial Hygiene Association, 20: 183-189 (1959).
- Devore, Jay L. Probability and Statistics for Engineering and the Sciences. California: Duxbury Press, 1991.
- Draxler, Roland R. "Determination of Atmospheric Diffusion Parameters," Atmospheric Environment, 10: 99-105, 1976.
- Draxler, Roland R. "Accuracy of Various Diffusion and Stability Schemes Over Washington, D.C.," Atmospheric Environment, 21: 491-499 (1987).
- Gifford, F. A. "Uses of Routine Meteorological Observations For Estimating Atmospheric Dispersion," Nuclear Safety, 2: 47-51 (1961).
- Gifford, F. A. "Turbulent Diffusion-Typing Schemes: A Review," Nuclear Safety, 17: 68-86 (1968).
- Golder, D. "Relations Among Stability Parameters in the Surface Layer," Boundary-Layer Meteorology, 3: 47-58 (1972).
- Hay, J.S. and F. Pasquill. "Diffusion From a Continuous Source in Relation to the Spectrum and Scale of Turbulence," in Atmospheric and Air Pollution. Ed. F. N. Frenkiel and P.A. Sheppard. New York: Academic Press, 1959.
- Holtslag, A.A.M. and A. P. Van Ulden. "A Simple Scheme for Daytime Estimates of the Surface Fluxes From Routine Weather Data," Journal of Climate and Applied Meteorology, 22: 517-529 (1983).
- Irwin, J. S. "Estimating Pluem Dispersion-A Recommended Generalization Scheme," Fourth Symposium on Turbulence, Diffusion, and Air Pollution. Nevada: American Meteorological Society, 1979.

- Irwin, J.J. "Estimating Plume Dispersion. A Comparison of Several Schemes," Journal of Climate and Applied Meteorology, 22: 92-114 (1983).
- McNeal, R.J. "NASA Global Tropospheric Experiment," Transcripts of the American Geophysical Union, 64: 561-562 (1983).
- Mitchell, A. Edgar Jr. "A Comparison of Short-Term Dispersion Estimates Resulting From Various Atmospheric Stability Classification Methods," Atmospheric Environment, 16: 765-774 (1982).
- Mitchell, A. Edgar Jr. and Keith Owen Timbre. "Atmospheric Stability Class From Horizontal Wind Fluctuation," Journal of The Air Pollution Control Association, 29: 1-16 (1979).
- Miller, C. W. "An Examination of Gaussian Plume Dispersion Parameters For Rough Terrain," Atmospheric Environment, 12: 1359-1364 (1978).
- Pasquill, F. "The Estimation of the Dispersion of Windborne Material," Meteorology Magazine, 90: 33-49 (1961).
- Pasquill, F. And F. B. Smith. "The Physical and Meteorological Basis For the Estimation of the Dispersion of Windborne Material" in Proceedings From The Second International Clean Air Congress. Ed. H.M England. New York: Academic Press, 1971.
- Pasquill, F. Atmospheric Dispersion Parameters in Gaussian Plume Modeling. North Carolina: U. S. Environmental Protection Agency, Office of Research and Development, 1976. Technical report EPA- 600/4-76-030h
- Pinker, R.T. and J.Z. Holland, "Dispersion Parameters over Forested Terrain," Journal of Applied Meteorology, 27: 1198-1217 (1988).
- Sedefian, Leon and Edward Bennett. "The Stability Determination Method: A Case For Uniform PSD Modeling," in The 2nd Joint Conference on Applications of Air Pollution Meteorology. New Orleans, LA: American Meteorological Society, 1980.
- Smith, F. B. "The Relations Between Pasquill Stability P and Kazanski-Monin Stability u (in Neutral and Unstable Conditions)," Atmospheric Environment, 13: 879-881 (1979).
- Tagliazucca, M. "An Atmospheric Diffusion Classification Scheme on the Kazanski-Monin Stability Parameter," Atmospheric Environment, 17: 2205-2211 (1983).

- Taylor, G. I. "Diffusion by Continuous Movement," Proceedings of the London Mathematical Society, 2: 196-202 (1921).
- Turner, D. Bruce, Workbook of Atmospheric Dispersion Estimates. Ohio: Public Health Service, Consumer Protection and Environmental Health Service, 1969. Publication No. 999-AP-26. 1969.
- Turner, D. Bruce. "Comparison of Three Methods for Calculating the Standard Deviation of the Wind Direction," Journal of Climate and Applied Meteorology, 25: 703-707 (1986).
- U.S. Atomic Energy Commission. Meteorology and Atomic Energy 1968. Oak Ridge: USAEC Division of Technical Information Extension, 1968.
- Yamartino, R. J. "A Comparison of Several "Single-Pass" Estimators of the Standard Deviation of Wind Passes," Journal of Climate and Applied Meteorology, 23: 1362-1366 (1984).
- Zoumakis, N.M. and A. G. Kelessis. "The Dependence of the Bulk Richardson Number on Stability in the Surface Layer," Boundary Layer Meteorology, 57: 407-414 (1991).

Vita

Capt John R. Lindell was born ~~May 1967 in Blue Island, Illinois~~. He graduated from Lake Central High School in St John, Indiana in 1985 and entered undergraduate study at Rose-Hulman Institute of Technology in Terre Haute, Indiana. He graduated with a Bachelor of Science degree in Mechanical Engineering on 27 May 1989. He received his commission the same day and entered active duty service on 15 August 1989 as a Civil Engineer officer at K. I. Sawyer Air Force Base, Michigan. After tours in Korea and Honduras, in May 1994 he entered the Engineering and Environmental Management program from the School of Engineering, Air Force Institute of Technology. He is presently assigned to the Environmental Management Section at Robins Air Force Base, Georgia. He is presently engaged to Miss Karen Babulak of Cincinnati, Ohio.

Permanent Address:

~~1499 Elm Court
Schererville, IN 46376~~

V-1

ADA307286

REPORT DOCUMENTATION PAGE

Form Approved
OMB No. 0704-0188

Public reporting burden for this collection of information is estimated to average 1 hour per response, including the time for reviewing instructions, searching existing data sources, gathering and maintaining the data needed, and completing and reviewing the collection of information. Send comments regarding this burden estimate or any other aspect of this collection of information, including suggestions for reducing this burden, to Washington Headquarters Services, Directorate for Information Operations and Reports, 1215 Jefferson Davis Highway, Suite 1204, Arlington, VA 22202-4302, and to the Office of Management and Budget, Paperwork Reduction Project (0704-0188), Washington, DC 20503.

1. AGENCY USE ONLY (Leave blank)		2. REPORT DATE December 1995	3. REPORT TYPE AND DATES COVERED Master's Thesis	
4. TITLE AND SUBTITLE THE EFFECTS OF VEGETATIVE CANOPIES ON ATMOSPHERIC DISPERSION			5. FUNDING NUMBERS	
6. AUTHOR(S) John R. Lindell, Capt, USAF				
7. PERFORMING ORGANIZATION NAME(S) AND ADDRESS(ES) Air Force Institute of Technology, WPAFB OH 45433-6583			8. PERFORMING ORGANIZATION REPORT NUMBER AFIT/GEE/ENP/95D-05	
9. SPONSORING / MONITORING AGENCY NAME(S) AND ADDRESS(ES)			10. SPONSORING / MONITORING AGENCY REPORT NUMBER	
11. SUPPLEMENTARY NOTES				
12a. DISTRIBUTION / AVAILABILITY STATEMENT Approved for public release; distribution unlimited			12b. DISTRIBUTION CODE	
13. ABSTRACT (Maximum 200 words) This research was conducted to improve our understanding of the effects of vegetative canopy-induced turbulence on the dispersion of air pollution. The computer model most often used to calculate atmospheric dispersion is the Gaussian plume model, which requires some method to compute the downwind dispersions coefficients. These coefficients are a parameterization of the atmospheric stability or the level of turbulence in the atmosphere. The Environmental Protection Agency's recommended parameterization scheme is the Pasquill-Gifford method. By comparing the Pasquill- Gifford method to the Modified Mitchell method using σ_z , the standard deviation of the horizontal wind fluctuations, the relative precision of each method is determined and their effects on a Gaussian model can be seen. Contrasting three sites with varying levels of vertical obstructions, the most effective method of measuring the turbulence level was determined to be the σ_z method. The meteorological data show that the wind direction fluctuates up to 50% more in a forested area when compared to an open field. This larger value translates to an increase in atmospheric turbulence at the forested site, In addition, the resulting output of the Gaussian model showed the forested site having a 3.5 times greater concentration than the open field, showing the effects of the increased turbulence and channeling of wind flow introduced by the forest canopy.				
14. SUBJECT TERMS Atmospheric Dispersion, Air Pollution, Vegetative Canopies Mechanical Turbulence, Atmospheric Stability			15. NUMBER OF PAGES 96	
			16. PRICE CODE	
17. SECURITY CLASSIFICATION OF REPORT Unclassified	18. SECURITY CLASSIFICATION OF THIS PAGE Unclassified	19. SECURITY CLASSIFICATION OF ABSTRACT Unclassified	20. LIMITATION OF ABSTRACT UL	

GENERAL INSTRUCTIONS FOR COMPLETING SF 298

The Report Documentation Page (RDP) is used in announcing and cataloging reports. It is important that this information be consistent with the rest of the report, particularly the cover and title page. Instructions for filling in each block of the form follow. It is important to *stay within the lines* to meet *optical scanning requirements*.

Block 1. Agency Use Only (Leave blank).

Block 2. Report Date. Full publication date including day, month, and year, if available (e.g. 1 Jan 88). Must cite at least the year.

Block 3. Type of Report and Dates Covered. State whether report is interim, final, etc. If applicable, enter inclusive report dates (e.g. 10 Jun 87 - 30 Jun 88).

Block 4. Title and Subtitle. A title is taken from the part of the report that provides the most meaningful and complete information. When a report is prepared in more than one volume, repeat the primary title, add volume number, and include subtitle for the specific volume. On classified documents enter the title classification in parentheses.

Block 5. Funding Numbers. To include contract and grant numbers; may include program element number(s), project number(s), task number(s), and work unit number(s). Use the following labels:

C - Contract	PR - Project
G - Grant	TA - Task
PE - Program Element	WU - Work Unit Accession No.

Block 6. Author(s). Name(s) of person(s) responsible for writing the report, performing the research, or credited with the content of the report. If editor or compiler, this should follow the name(s).

Block 7. Performing Organization Name(s) and Address(es). Self-explanatory.

Block 8. Performing Organization Report Number. Enter the unique alphanumeric report number(s) assigned by the organization performing the report.

Block 9. Sponsoring/Monitoring Agency Name(s) and Address(es). Self-explanatory.

Block 10. Sponsoring/Monitoring Agency Report Number. (If known)

Block 11. Supplementary Notes. Enter information not included elsewhere such as: Prepared in cooperation with...; Trans. of...; To be published in.... When a report is revised, include a statement whether the new report supersedes or supplements the older report.

Block 12a. Distribution/Availability Statement. Denotes public availability or limitations. Cite any availability to the public. Enter additional limitations or special markings in all capitals (e.g. NOFORN, REL, ITAR).

DOD - See DoDD 5230.24, "Distribution Statements on Technical Documents."

DOE - See authorities.

NASA - See Handbook NHB 2200.2.

NTIS - Leave blank.

Block 12b. Distribution Code.

DOD - Leave blank.

DOE - Enter DOE distribution categories from the Standard Distribution for Unclassified Scientific and Technical Reports.

NASA - Leave blank.

NTIS - Leave blank.

Block 13. Abstract. Include a brief (*Maximum 200 words*) factual summary of the most significant information contained in the report.

Block 14. Subject Terms. Keywords or phrases identifying major subjects in the report.

Block 15. Number of Pages. Enter the total number of pages.

Block 16. Price Code. Enter appropriate price code (*NTIS only*).

Blocks 17. - 19. Security Classifications. Self-explanatory. Enter U.S. Security Classification in accordance with U.S. Security Regulations (i.e., UNCLASSIFIED). If form contains classified information, stamp classification on the top and bottom of the page.

Block 20. Limitation of Abstract. This block must be completed to assign a limitation to the abstract. Enter either UL (unlimited) or SAR (same as report). An entry in this block is necessary if the abstract is to be limited. If blank, the abstract is assumed to be unlimited.